Formation of Jets by Baroclinic Turbulence

BRIAN F. FARRELL

Department of Earth and Planetary Sciences, Harvard University, Cambridge, Massachusetts

PETROS J. IOANNOU

Department of Physics, National and Capodistrian University of Athens, Athens, Greece

(Manuscript received 4 September 2007, in final form 7 March 2008)

ABSTRACT

Turbulent fluids are frequently observed to spontaneously self-organize into large spatial-scale jets; geophysical examples of this phenomenon include the Jovian banded winds and the earth's polar-front jet. These relatively steady large-scale jets arise from and are maintained by the smaller spatial- and temporal-scale turbulence with which they coexist. Frequently these jets are found to be adjusted into marginally stable states that support large transient growth. In this work, a comprehensive theory for the interaction of jets with turbulence, stochastic structural stability theory (SSST), is applied to the two-layer baroclinic model with the object of elucidating the physical mechanism producing and maintaining baroclinic jets, understanding how jet amplitude, structure, and spacing is controlled, understanding the role of parameters such as the temperature gradient and static stability in determining jet structure, understanding the phenomenon of abrupt reorganization of jet structure as a function of parameter change, and understanding the general mechanism by which turbulent jets adjust to marginally stable states supporting large transient growth.

When the mean thermal forcing is weak so that the mean jet is stable in the absence of turbulence, jets emerge as an instability of the coupled system consisting of the mean jet dynamics and the ensemble mean eddy dynamics. Destabilization of this SSST coupled system occurs as a critical turbulence level is exceeded. At supercritical turbulence levels the unstable jet grows, at first exponentially, but eventually equilibrates nonlinearly into stable states of mutual adjustment between the mean flow and turbulence. The jet structure, amplitude, and spacing can be inferred from these equilibria.

With weak mean thermal forcing and weak but supercritical turbulence levels, the equilibrium jet structure is nearly barotropic. Under strong mean thermal forcing, so that the mean jet is unstable in the absence of turbulence, marginally stable highly nonnormal equilibria emerge that support high transient growth and produce power-law relations between, for example, heat flux and temperature gradient. The origin of this power-law behavior can be traced to the nonnormality of the adjusted states.

As the stochastic excitation, mean baroclinic forcing, or the static stability are changed, meridionally confined jets that are in equilibrium at a given meridional wavenumber abruptly reorganize to another meridional wavenumber at critical values of these parameters.

The equilibrium jets obtained with this theory are in remarkable agreement with equilibrium jets obtained in simulations of baroclinic turbulence, and the phenomenon of discontinuous reorganization of confined jets has important implications for storm-track reorganization and abrupt climate change.

1. Introduction

Coherent jets that are not forced at the jet scale are often observed in turbulent flows, with a familiar geophysical-scale example being the banded winds of the gaseous planets (Ingersoll 1990; Vasavada and Showman 2005; Sánchez-Lavega et al. 2008). In the earth's midlatitude troposphere, the polar-front jets are eddy driven (Jeffreys 1933; Lee and Kim 2003). The earth's equatorial stratosphere is characterized by the eddy-driven quasi-biennial oscillation (QBO) jet (Baldwin et al. 2001); the equatorial ocean supports eddy-driven equatorial deep jets (Muench and Kunze 1994). The midlatitude ocean also supports alternating eddy-driven zonal jets, which are seen both in observations

Corresponding author address: Brian Farrell, Harvard University, Department of Earth and Planetary Sciences, Geological Museum 452, 24 Oxford Street, Cambridge, MA 02138.
E-mail: farrell@seas.harvard.edu

DOI: 10.1175/2008JAS2611.1

(Maximenko et al. 2005) and in models (Nakano and Hasumi 2005; Richards et al. 2006). The phenomenon of spontaneous jet organization in turbulence has been extensively investigated in observational and in theoretical studies (Rhines 1975; Williams 1979, 2003; Panetta 1993; Nozawa and Yoden 1997; Huang and Robinson 1998; Manfroi and Young 1999; Vallis and Maltrud 1993; Cho and Polvani 1996; Galperin et al. 2004; Lee 2005; Kaspi and Flierl 2007) as well as in laboratory experiments (Krishnamurti and Howard 1981; Read et al. 2004, 2007). The mechanism by which eddies maintain jets against surface drag is upgradient momentum flux produced by the continuous spectrum of shear waves as distinct from the discrete set of jet modes (Huang and Robinson 1998; Panetta 1993; Vallis and Maltrud 1993). This upgradient momentum transfer mechanism maintains jets in barotropic flows (Huang and Robinson 1998) and is also an important component of the eddy forcing maintaining baroclinic jets (Panetta 1993; Williams 2003). However, baroclinic jet structure is additionally influenced by eddy heat fluxes and secondary circulations as well as by externally imposed mean thermal forcing.

A characteristic property of mean jets in strong synoptic-scale turbulence is marginal stability coexisting with robust transient growth (Farrell 1985; Hall and Sardeshmukh 1998; Sardeshmukh and Sura 2007). In the case of the midlatitude jet, this marginally stable state is traditionally referred to as a baroclinically adjusted state after its original description by Stone (1978), who drew attention to the proximity of mean jet states to the classical two-layer model stability boundary. It is now recognized that observed and simulated marginally stable jets frequently exceed this necessary condition for baroclinic instability that would apply to the stability of a dissipationless and meridionally constant shear. This is no contradiction of marginal jet stability because a correct assessment of jet stability requires an eigenanalysis in which proper account is taken of dissipation, quantization by boundaries, and jet structure, particularly the stabilization effect of meridional shear (Ioannou and Lindzen 1986; James 1987; Roe and Lindzen 1996; DelSole and Farrell 1996; Hall and Sardeshmukh 1998).

The recognition, in both observations and simulations, of adjustment to marginal stability in baroclinic turbulence resulted in application of a variety of theoretical approaches to understanding this phenomenon. This effort was motivated in part by the fact that baroclinic adjustment is a fundamental problem in the theory of baroclinic turbulence but also by its implications for flux parameterization in climate models. These theoretical approaches include adjustment by the unstable modes themselves (Stone 1978; Held 1978; Lindzen and Farrell 1980; Gutowski 1985; Gutowski et al. 1989; Stone and Branscome 1992; Lindzen 1993; Welch and Tung 1998; Zurita-Gotor and Lindzen 2004a,b; Schneider and Walker 2006) and scaling arguments for turbulent transport (Green 1970; Stone 1972, 1974; Held 1978; Held and Larichev 1996; Held 1999; Lapeyre and Held 2003; Zurita-Gotor 2007). Baroclinic turbulence is additionally characterized by power-law behavior of fluxes as a function of variables controlling stability such as the temperature gradient (Held and Larichev 1996; Barry et al. 2002; Zurita-Gotor 2007) and a theory for baroclinic turbulence should account also for these power-law relations.

A model commonly employed for theoretical studies of baroclinic turbulence is the two-layer model in a doubly periodic domain (Haidvogel and Held 1980; Panetta 1993). This model maintains a constant mean shear. Consequently, the Phillips (1954) two-layer model stability criterion, if it is calculated using the mean shear, cannot be changed by fluxes in this model. However, it does not follow that baroclinic adjustment does not occur. In the two-layer model, adjustment to marginal stability can result from a combination of dissipation, quantization by boundaries, and meridional confinement associated with the spontaneous emergence of alternating jets.

We show how turbulent atmospheric jets are adjusted to stable but highly amplifying mean states. Analogous behavior often arises when a feedback controller is imposed to stabilize multidimensional mechanical or electronic systems and attempts to suppress the nonnormal growth in such systems gave rise to robust control theory (Zhou and Doyle 1998). It is commonly held that stable but fragile equilibria arise primarily as a consequence of a design process (Bobba et al. 2002). We find that the state of high nonnormality together with marginal stability is inherent to strongly turbulent eddy-driven baroclinic jets because turbulence maintains flow stability with a naturally occurring feedback controller. A fundamental advantage of our theory is that it clearly reveals this feedback stabilization process and how it places the system in a stable but highly amplifying state.

Excitation of the turbulent eddies can be traced either to exogenous processes such as convection, as in the case of the Jovian jets, or to endogenous sources such as wave–wave interaction, as in the case of the earth's polar-front jet. These processes have short temporal and spatial correlation scales compared with the jet temporal and spatial scales, and their effect in forcing the synoptic-scale wave field can be approximated as stochastic (Sardeshmukh and Sura 2007). The central

component of a theory for the dynamics of jets in baroclinic turbulence—namely, the method to obtain the structure of the turbulence and the associated fluxes given the jet—is provided by stochastic turbulence modeling (Farrell and Ioannou 1993c, 1994, 1995, 1996; DelSole and Farrell 1995, 1996; DelSole 1996; Newman et al. 1997; Whitaker and Sardeshmukh 1998; Zhang and Held 1999; DelSole 2004b). Once these fluxes are known, the equilibrium states of balance among the large-scale thermal forcing, the dissipation, and the ensemble mean turbulent flux divergences can be determined; this is the method of SSST.[1] (Farrell and Ioannou 2003, 2007). The interaction between the large-scale jet structure and the field of eddy turbulence is nonlinear and results in a nonlinear trajectory for the jet and the ensemble mean eddy field associated with it, which often tends to an equilibrium and sometimes to a limit cycle, but under extraordinary conditions is chaotic.

There are three length scales in the baroclinic dynamics of the two-layer model on a β plane: the scale imposed by the boundaries; the Rossby radius $L_R = NH/f_0$ (in which f_0 is the Coriolis parameter, N the buoyancy frequency, and H the depth of the fluid); and the β scale, $L_\beta = \sqrt{U/\beta}$, where U is a characteristic velocity and β is the meridional gradient of the Coriolis parameter. This U may be taken as the characteristic velocity of the jet or of the eddies; when the rms eddy velocity is taken for U, this length is proportional to the Rhines radius. When U is the jet velocity, it is the length scale for which planetary and shear vorticity gradients are comparable.

We find in the presence of turbulence, and even in the absence of an imposed mean thermal forcing, that there is a linear instability of the coupled turbulence–mean flow system giving rise to zonal jets. This jet-forming instability is an example of a new class of instability in fluid dynamics; it is an emergent instability that arises from the interaction between the mean flow and the turbulence. The modal jet perturbation growth rate is exponential because the jet modes organize the turbulence field to produce fluxes proportional in magnitude and consistent in structure with the jet mode.

It is instructive to consider this jet forming instability as a function of the strength of the stochastic excitation, the mean thermal forcing, the static stability, and dissipation.

With sufficiently energetic homogeneous stochastic excitation and no mean thermal forcing, the zonal jets that emerge spontaneously are nearly barotropic. If the stochastic excitation is not too strong, these jets equilibrate nonlinearly with a nearly sinusoidal barotropic structure. However, as the stochastic excitation is increased the nonlinearly balanced jets increase in amplitude and encroach on eddy stability boundaries. This results in modification of the jet structure as SSST fixed-point equilibria enforce stability of the jet to eddy perturbations because eddy fluxes diverge at stability boundaries.[2] To avoid eddy instability, the jets become increasingly east–west asymmetric, with the westward jet equilibrating primarily barotropically at the Rayleigh–Kuo scale, which results in emergence of meridional jet spacing with the β scale L_β.

When mean thermal forcing is imposed, baroclinic equilibria are found. Under strong stochastic excitation, the eastward part of these jet equilibria become substantially baroclinic while at the same time becoming sufficiently narrow meridionally so that perturbation eddy stability is maintained by meridional confinement (Ioannou and Lindzen 1986; James 1987; Roe and Lindzen 1996). The westward parts of these jets equilibrate near the Rayleigh–Kuo boundary with more nearly barotropic structure.

Although jet equilibria with marginal stability have been recognized as characteristic of baroclinic turbulence and meridional confinement has been implicated in their stabilization, our theory is far more specific than a diagnostic in that it provides a method for predicting the precise structure of the equilibria. These equilibria are preferred states in the sense of being precisely known marginally stable structures maintained by the turbulence. However, their structure varies either continuously or discontinuously as a function of parameters influencing stability, such as the static stability or mean thermal forcing, so that no single preferred structure can be said to characterize the adjusted state.

If the jets are quantized by meridional boundaries, as would be the case for a planet of finite radius, a discontinuous reorganization of structure is induced at threshold parameter values for which stable equilib-

[1] The term "stochastic structural stability theory" was chosen to connote analysis of both the equilibria emergent from the cooperative interaction between turbulence and mean flows and the structural stability of these equilibria with parameter change.

[2] It is logically necessary that exponential eddy instabilities be equilibrated in some manner. The mechanism of equilibration in our model, and we believe the primary mechanism in atmospheric jets generally, is through modification of the mean jet structure by the eddy fluxes. In our quasigeostrophic model this modification is necessarily confined to changes in jet velocity and attendant horizontal temperature gradients, but more generally modification of static stability must be involved in some manner that remains to be investigated using a nongeostrophic model.

rium states with the extant marginally stable wavenumber cease to exist. This provides an instructive example of the general phenomenon of eddy-driven jets appearing and disappearing discontinuously as a function of slow parameter change (Lee 1997; Farrell and Ioannou 2003; Robinson 2006). Understanding the physical mechanism determining the structure the eddy-driven jet is a fundamental geophysical fluid dynamics problem with important climate implications because discontinuous reorganization of eddy-driven jets can alter both climate statistics, by altering storm tracks and the source regions associated with isotopic signatures (Alley et al. 1993; Fuhrer et al. 1999; Wunsch 2003), and the climate itself, by changing the latitude of surface stresses and associated oceanic upwelling (Toggweiler et al. 2006). This mechanism for abrupt change of climate and climate statistics arising from storm-track reorganization joins the short list of reorganization of thermohaline ocean circulations (Weaver et al. 1991), ice sheet instability (MacAyeal 1993), and sea ice switches (Gildor and Tziperman 2003; Li et al. 2005) as possible mechanisms for explaining the observed record of abrupt climate change.

In this work we study the structure and dynamics of jets in baroclinic turbulence by joining the equation governing ensemble mean eddy statistics with the equation for the zonal mean to form a coupled wave–mean flow evolution system. This nonlinear coupled equation system is the basic tool of SSST analysis and we have applied it previously to the study of barotropic jets (Farrell and Ioannou 2003, 2007).

2. Dynamics of the zonal average velocity in turbulent flows

a. Formulation

A theory for jet dynamics in turbulent flow was developed in Farrell and Ioannou (2003) and applied to the problem of the formation of jets in barotropic turbulence in Farrell and Ioannou (2007). Here we provide a brief review of the salient ideas of this theory in the context of baroclinic jets, which is the focus of this work.

Consider a turbulent rotating two-layer baroclinic fluid on a β plane, and let $U_{1,2}(y, t)$ be the latitudinally (y) and time (t) dependent mean velocities of the upper (denoted as 1) and lower (denoted as 2) layers, the mean being taken in the zonal (x) direction. The barotropic (denoted +) and baroclinic (denoted −) mean flows, defined as

$$U^+ = \frac{U_1 + U_2}{2} \quad \text{and} \quad U^- = \frac{U_1 - U_2}{2}, \tag{1}$$

obey the following evolution equations (DelSole and Farrell 1996; Vallis 2006):

$$U^+_t = -\frac{\bar{r}_2}{2}(U^+ - U^-) + F^+ \quad \text{and} \tag{2}$$

$$(D^2 - 2\lambda^2)U^-_t = \frac{\bar{r}_2}{2}D^2(U^+ - U^-) - 2r_R\lambda^2(U^-_R - U^-) + D^2F^-, \tag{3}$$

in which the term proportional to $\bar{r}_2$ represents linear damping of the mean flow at the lower layer to a state of rest (we assume no Rayleigh damping in the upper layer); the term proportional to r_R represents linear relaxation of the baroclinic flow to the imposed baroclinic flow U^-_R; and the terms F^+ and F^- (explicit forms given later) represent the forcing of the zonal flow by the eddies. The nondimensional Rossby radius of deformation is $L_R = 1/\lambda = NH/fL$, where L is the horizontal scale, H the height of each layer, N the static stability, and f the Coriolis parameters. The operator $D^2 \equiv \partial^2/\partial y^2$.

The equations for the mean flow are written in the compact form

$$\frac{d\mathbf{U}}{dt} = \mathbf{G}\mathbf{U} + \mathbf{H}, \tag{4}$$

in which the $\mathbf{U}$ is the full mean state velocity vector

$$\mathbf{U} \equiv \begin{pmatrix} U^+ \\ U^- \end{pmatrix}; \tag{5}$$

$\mathbf{G}$ is the linear dissipation operator

$$\mathbf{G} = \begin{pmatrix} G_{11} & G_{12} \\ G_{21} & G_{22} \end{pmatrix}, \tag{6}$$

with components

$$G_{11} = -\frac{\bar{r}_2}{2}, \tag{7a}$$

$$G_{12} = +\frac{\bar{r}_2}{2}, \tag{7b}$$

$$G_{21} = (D^2 - 2\lambda^2)^{-1}\left(\frac{\bar{r}_2}{2}D^2\right), \quad \text{and} \tag{7c}$$

$$G_{22} = (D^2 - 2\lambda^2)^{-1}\left(-\frac{\bar{r}_2}{2}D^2 + 2r_R\lambda^2\right); \tag{7d}$$

and the mean flow forcing $\mathbf{H}$ is composed of the eddy forcing and relaxation toward the radiative equilibrium thermal wind U^-_R; that is,

$$\mathbf{H} \equiv \begin{bmatrix} F^+ \\ (D^2 - 2\lambda^2)^{-1}(D^2F^- - 2r_R\lambda^2U^-_R) \end{bmatrix}. \tag{8}$$

The eddy forcing of the mean flow is expressed in terms of the barotropic and baroclinic eddy streamfunction (DelSole and Farrell 1996; Vallis 2006) as

$$F^+ = \overline{\psi_x^+ \psi_{yy}^+ + \psi_x^- \psi_{yy}^-} \quad \text{and} \tag{9a}$$

$$F^- = \overline{\psi_x^+ \psi_{yy}^- + \psi_x^- \psi_{yy}^+ - 2\lambda^2 \psi_x^+ \psi^-}. \tag{9b}$$

The overbar denotes a zonal average and the perturbation velocities are related to the streamfunctions $\psi^\pm$ as

$$u^\pm = -\psi_y^\pm \quad \text{and} \quad v^\pm = \psi_x^\pm. \tag{10}$$

The perturbation streamfunctions are expanded in a Fourier sum of zonal harmonics:

$$\psi^\pm(x, y, t) = \sum_k \psi_k^\pm(y, t) e^{ikx}. \tag{11}$$

The zonal average $\overline{ab}$ of the product of two sinusoidally varying fields $\hat{a}e^{ikx}$ and $\hat{b}e^{ilx}$ is $\mathrm{Re}(\hat{a}\hat{b}^*)\delta_{kl}/2$ (* denotes complex conjugate). Using this property, the eddy forcings [(9a), (9b)] are expressed in terms of the eddy streamfunction Fourier amplitudes as

$$F^+ = -\sum_k \frac{k}{2} \mathrm{Im}(\psi_k^+ D^2 \psi_k^{+*} + \psi_k^- D^2 \psi_k^{-*}) \quad \text{and} \tag{12a}$$

$$F^- = -\sum_k \frac{k}{2} \mathrm{Im}(\psi_k^+ D^2 \psi_k^{-*} + \psi_k^- D^2 \psi_k^{+*} - 2\lambda^2 \psi_k^+ \psi_k^{-*}). \tag{12b}$$

Each Fourier component of the perturbation streamfunction evolves according to the stochastically excited linear equation

$$\frac{d}{dt}\begin{pmatrix} \psi_k^+ \\ \psi_k^- \end{pmatrix} = \mathbf{A}_k(\mathbf{U})\begin{pmatrix} \psi_k^+ \\ \psi_k^- \end{pmatrix} + \mathbf{P}_k\begin{pmatrix} \xi(t)^+ \\ \xi(t)^- \end{pmatrix}. \tag{13}$$

In (13), the second term on the rhs represents stochastic excitation and in the first term the autonomous linear operator of the perturbation dynamics is

$$\mathbf{A}_k(\mathbf{U}) = \begin{bmatrix} A_k^+(U^+) & A_k^+(U^-) \\ A_k^-(U^+) & A_k^-(U^-) \end{bmatrix}, \tag{14}$$

in which the individual linear operators are

$$A_k^+(U^+) = \Delta^{-1}[-ikU^+\Delta - ik(\beta - D^2U^+)] - r^+ - r_{\mathrm{eff}}, \tag{15a}$$

$$A_k^+(U^-) = \Delta^{-1}(-ikU^-\Delta + ikD^2U^-) - r^-, \tag{15b}$$

$$A_k^-(U^+) = (\Delta - 2\lambda^2)^{-1}[-ikU^-(\Delta + 2\lambda^2) + ikD^2U^- - r^-\Delta], \quad \text{and} \tag{15c}$$

$$A_k^-(U^-) = (\Delta - 2\lambda^2)^{-1}[-ikU^+(\Delta - 2\lambda^2) + (\beta - D^2U^+) - r^+\Delta + 2r_R\lambda^2] - r_{\mathrm{eff}}, \tag{15d}$$

where $\Delta \equiv D^2 - k^2$ is the Laplacian and Δ^{-1} is the inverse of the Laplacian in which the appropriate lateral boundary conditions have been incorporated. In writing (13) we have included the linear operator parameterization of the nonlinear terms in the complete perturbation equation as stochastic excitation and added dissipation in the form of linear damping of the streamfunction at rate r_{eff} (Farrell and Ioannou 1993b, 1996; DelSole and Farrell 1996; Newman et al. 1997; DelSole 2004b). The coefficients $r^\pm$ are the linear damping rates of the barotropic and baroclinic streamfunction, respectively.

The stochastic excitation is given by

$$\mathbf{P}_k = \alpha_k \begin{bmatrix} \Delta^{-1} & 0 \\ 0 & (\Delta - 2\lambda^2)^{-1} \end{bmatrix} \begin{bmatrix} \mathbf{W}^+(y) & 0 \\ 0 & \mathbf{W}^-(y) \end{bmatrix}. \tag{16}$$

The stochastic excitation of the potential vorticity represented by (16) is Δ correlated in time and spatially correlated by $\mathbf{W}^\pm(y)$. The scalar coefficient α_k is chosen so that each perturbation wavenumber is forced with equal energy.

The continuous operators are discretized and the dynamical operator is approximated by a finite dimensional matrix. The state $\psi^\pm(k)$ is represented by a column vector with entries for the complex value of the streamfunction at collocation points. In this approximation, $\mathbf{W}$ represents the spatial (y) correlation in the stochastic excitation. Care must be taken that the structure of excitation matrix $\mathbf{W}$ does not bias the response. We select $\mathbf{W}$ matrices producing Gaussian autocorrelation function about the level of excitation y_i proportional to $\exp[-(y - y_i)^2/\delta^2]$ so that δ controls the correlation distance in y. This forcing matrix is the same for all zonal wavenumbers.

If the layers are excited equally, the stochastic excitation of the time dependence of the barotropic $\xi^+(t)$ and baroclinic $\xi^-(t)$ components is equal and statistically independent so that

$$\langle \xi^+(t) \xi^{-\dagger}(t) \rangle = \mathbf{0}, \tag{17}$$

where the angled brackets indicate the ensemble average (i.e., an average over realizations of the forcing). We choose each of the excitations to be delta correlated with zero mean and unit variance; thus,

$$\langle \xi^+(t) \rangle = \langle \xi^-(t) \rangle = 0, \quad \text{and}$$
$$\langle \xi^+(t) \xi^{+\dagger}(s) \rangle = \langle \xi^-(t) \xi^{-\dagger}(s) \rangle = \mathbf{I}\delta(t - s), \tag{18}$$

where $\mathbf{I}$ is the identity matrix. If only the upper layer is forced, then the barotropic and baroclinic forcing are taken equal to $\xi^+(t)$.

The system consisting of (4) and (13) describes the dynamics of a single realization of a stochastically ex-

cited wave field interacting with the jet. This system results in strong fluctuations in jet structure. However, there are usually many independently excited waves simultaneously interacting with the jet, so the fluctuations in jet structure are suppressed by the ensemble averaging of these independently excited wave fields. With this assumption of ensemble average wave forcing, the time evolution of the ensemble average covariance matrix of the perturbation field

$$\mathbf{C}_k = \begin{bmatrix} \mathbf{C}_k^+ & \mathbf{C}_k^\pm \\ (\mathbf{C}_k^\pm)^\dagger & \mathbf{C}_k^- \end{bmatrix}, \tag{19}$$

with $\mathbf{C}_k^+ = \langle \psi_k^+ \psi_k^{+\dagger} \rangle$, $\mathbf{C}_k^- = \langle \psi_k^- \psi_k^{-\dagger} \rangle$, and $\mathbf{C}_k^\pm = \langle \psi_k^+ \psi_k^{-\dagger} \rangle$, obeys the deterministic equation

$$\frac{d\mathbf{C}_k}{dt} = \mathbf{A}_k(\mathbf{U})\mathbf{C}_k + \mathbf{C}_k\mathbf{A}_k^\dagger(\mathbf{U}) + \mathbf{Q}_k, \quad \text{with} \tag{20}$$

$$\mathbf{Q}_k = |\alpha_k|^2 \begin{bmatrix} \Delta^{-1}\mathbf{W}^+(\mathbf{W}^+)^\dagger\Delta^{-1\dagger} & 0 \\ 0 & (\Delta - 2\lambda^2)^{-1}\mathbf{W}^-(\mathbf{W}^-)^\dagger(\Delta - 2\lambda^2)^{-1\dagger} \end{bmatrix}, \tag{21}$$

the spatial covariance matrix for equal stochastic excitation of both layers (in the case of excitation limited to the upper layer, $\mathbf{Q}_k$ is modified appropriately). For our purposes, $\mathbf{Q}_k$ includes all the relevant characteristics of the stochastic excitation; the meridional distribution of the forcing is given by the diagonal elements of this matrix and the autocorrelation function by the rows.

The ensemble mean baroclinic and barotropic eddy forcings [(12a), (12b)] are expressed in terms of the covariances as

$$\langle F^+ \rangle = \sum_k -\frac{k}{2}\,\mathrm{diag}[\mathrm{Im}(\mathbf{C}_k^+ + \mathbf{C}_k^-)D^{2\dagger}], \tag{22a}$$

$$\langle F^- \rangle = \sum_k -\frac{k}{2}\,\mathrm{diag}\{\mathrm{Im}[(\mathbf{C}_k^\pm + \mathbf{C}_k^{\pm\dagger})D^{2\dagger} - 2\lambda^2\mathbf{C}_k^\pm]\}, \tag{22b}$$

and these ensemble means of zonal average forcings are introduced in place of the single realization of zonal average forcing in (9a) and (9b).

In this limit, the evolution equation for the covariance [(20)], the equation for the ensemble mean eddy forcing [(22a), (22b)] and the equation for the barotropic and baroclinic mean zonal flow [(4)] define a closed autonomous nonlinear system for the evolution of the mean flow under the influence of its consistent field of turbulent eddies. This system is energetically consistent and globally stable. For typical earth values of mean baroclinic forcing, there is a small energy input by the stochastic forcing, which can be accounted for in the energy balance by a slight increase in dissipation, whereas the dominant balance is between energy extracted from the mean by baroclinic processes and energy lost to frictional dissipation. Typically the equilibrium solutions of this system are steady mean flows maintained with constant structure by eddy forcing, although limit cycle and chaotic trajectories are found for some parameter values (Farrell and Ioannou 2003).

This ideal limit in which the ensemble average eddy forcing is taken is of particular interest because in this limit, although the effect of the ensemble average turbulent fluxes is retained in the solution, the fluctuations associated with the turbulent eddies are suppressed by the averaging and the coupled jet–turbulence dynamics becomes deterministic. In this limit the mean zonal flow equilibria emerge with great clarity. This ideal limit is approached when the autocorrelation scale of the perturbation field l is much smaller than the zonal extent L of the domain. In that case, taking the zonal average is equivalent to averaging $N = O(L/l)$ statistically independent realizations of the forcing, which converges to the ensemble average as $N \to \infty$ (Farrell and Ioannou 2003). Examples of physical systems in which this limit applies include the Jovian upper atmosphere and the solar convection zone, both forced by relatively small-scale convection. An experiment in which a jet emerged from rather coarse-grained turbulent convection was reported by Krishnamurti and Howard (1981). When this large ensemble limit is not approached sufficiently closely, the system exhibits stochastic fluctuations about the ideal equilibrium. A physical system that exhibits such behavior is the earth's polar jet, in which the number of independent cyclones around a latitude circle is at most order 10 so that, while the underlying order is revealed by the ideal dynamics, the observed zonal jet exhibits stochastic fluctuations about the ideal jet (Farrell and Ioannou 2003).

A limitation of our analysis is the assumption that the stochastic excitation is independent of the mean and eddy fields. Although for the Jovian atmosphere this is probably a good assumption, because the stochastic excitation is thought to arise from internally generated convection, it is a crude assumption for the earth's polar jet, in which the excitation is influenced by the jet structure and eddy amplitude itself. Obtaining the stochastic excitation consistent with the turbulence supported by

a jet is equivalent to obtaining a closure of the turbulent system, and progress on this problem has been made (DelSole and Farrell 1996; DelSole 1999). Although an attractive avenue for future study, such a closure is not necessary for understanding the basic dynamics underlying emergence of zonal jets in turbulence; in the interest both of simplicity and of clarity of exposition, we for the present retain a spatially uniform stochastic excitation.

b. *Scaling of the equations, boundary conditions, and parameters*

The equations are nondimensionalized, using the earth day for the time scale, $t_d = 1$ day, and $L = 10^6$ m for the length scale so that the velocity scale is $L/t_d = 11.6\ \mathrm{m\ s^{-1}}$. The calculations are performed in a doubly periodic domain with width $L_y = 20$ units in the meridional direction. This doubly periodic model was introduced by Haidvogel and Held (1980) and used in the work of Panetta (1993) and Held and Larichev (1996). The size of the domain has been selected to be wide enough to accommodate a number of jets; however, quantization effects do become important, as will be shown below. The calculations use typically 64-point discretization in the meridional direction and 14 waves in the zonal direction, consisting of global zonal wavenumbers 1 to 14 in a periodic zonal domain of nondimensional length $L_x = 40$.

The strength of the stochastic excitation $\mathbf{Q}_k$ is measured by the forcing density $\mathcal{F} = \mathrm{trace}(\mathbf{M}\mathbf{Q}_k)/n$, where $\mathbf{M}$ is the energy metric

$$\mathbf{M} = -\frac{1}{2n}\begin{bmatrix} \Delta & 0 \\ 0 & (\Delta - 2\lambda^2) \end{bmatrix}, \tag{23}$$

defined so that $(\psi_k^+, \psi_k^-)\mathbf{M}(\psi_k^+, \psi_k^-)^\dagger$ is the total energy per unit mass of state (ψ_k^+, ψ_k^-) at each zonal wavenumber k, and n is the number of discretization points in the meridional direction. For convenience, the stochastic excitation will at times be expressed in dimensional units ($\mathrm{mW\ kg^{-1}}$).

Unless otherwise specified, friction parameters for the perturbation dynamics are $r_R = 1/15$, $r_2 = 1/5$, and $r_{\mathrm{eff}} = 1/20$. For the mean dynamics, $\bar{r}_2 = 1/5$ and viscosity $\nu = (\delta y)^2$, where δy is the grid size. The Froude number in most of the calculations is $\lambda^2 = 1/L_R^2 = 1$.

For simplicity and to facilitate interpretation, we impose meridionally homogeneous stochastic excitation and meridionally constant radiative equilibrium forcing with shear:

$$U_1 - U_2 = 2U_R^- = \frac{R\Delta T}{f_0}\frac{t_d}{20L^2}, \tag{24}$$

where ΔT is the temperature difference across 10^4 km, $f_0 = 10^{-4}\ \mathrm{s^{-1}}$ is the Coriolis parameter, and $R = 287\ \mathrm{J\ (kg\ K)^{-1}}$ is the gas constant. This constant shear flow becomes baroclinically unstable when $\Delta T > \Delta T_c$, which with the above dissipation parameters is $\Delta T_c = 28.3\ \mathrm{K\ (10^4\ km)^{-1}}$. An important parameter is the criticality defined as

$$\xi = 4(U_1 - U_2)/(\beta\lambda^2). \tag{25}$$

Supercriticality (i.e., $\xi > 1$) implies exponential instability of the inviscid two-layer model for meridionally constant flows according to the Phillips (1954) criterion. The criticality is not a criterion for instability of realistic flows, which are generally both meridionally varying and dissipative. Because of the presence of dissipation in the example above, the critical temperature gradient for instability $\Delta T_c = 28.3\ \mathrm{K\ (10^4\ km)^{-1}}$ corresponds to criticality $\xi = 2.03$.

3. Stability analysis of the ensemble mean coupled system

Recall that in the ensemble mean limit the eddy/mean jet system is governed by the coupled equations

$$\frac{d\mathbf{C}_k}{dt} = \mathbf{A}_k(\mathbf{U})\mathbf{C}_k + \mathbf{C}_k\mathbf{A}_k(\mathbf{U})^\dagger + \mathbf{Q}_k \quad \text{and} \tag{26a}$$

$$\frac{d\mathbf{U}}{dt} = \mathbf{G}\mathbf{U} + \mathbf{H}. \tag{26b}$$

The equilibria of this set of equations consist of an equilibrium velocity $\mathbf{U}^E$ and an associated equilibrium perturbation covariance $\mathbf{C}^E$ satisfying

$$\mathbf{A}_k(\mathbf{U}^E)\mathbf{C}_k^E + \mathbf{C}_k^E\mathbf{A}_k(\mathbf{U}^E)^\dagger = -\mathbf{Q}_k, \tag{27a}$$

$$\mathbf{G}\mathbf{U}^E + \mathbf{H} = 0. \tag{27b}$$

If stable, these equilibria may be found by forward integration of the coupled Eqs. (26a) and (26b); otherwise, a root finder must be employed.

Two distinct concepts of jet stability arise in connection with these equilibria. The first is the familiar eddy perturbation stability determined by analysis of the operator $\mathbf{A}^E$. An equilibrium mean flow $\mathbf{U}^E$ is by necessity stable in this sense because otherwise the eddy variance would diverge. The converse, however, is not true; the stability of $\mathbf{A}^E$ does not imply the stability of the equilibrium ($\mathbf{U}^E$, $\mathbf{C}^E$), and there is a new stability concept arising from the interaction of the jet with its consistent eddy flux divergences. The stability of the coupled system (26a) and (26b) is determined by analysis of the operator that governs the perturbation dynamics of its equilibria, as discussed in Farrell and Ioannou (2003,

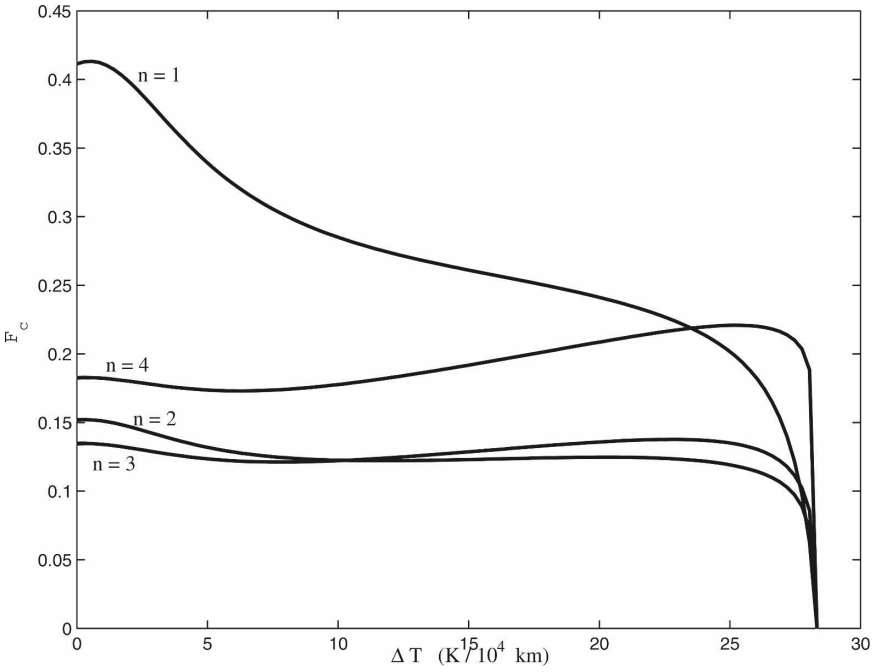

FIG. 1. The critical value of stochastic excitation $\mathcal{F}_c$ (m W kg^{-1}) required to structurally destabilize the baroclinic jet in thermal wind balance with mean thermal forcing ΔT [K (10^4 km)$^{-1}$]. The different curves correspond to the critical stochastic excitation $\mathcal{F}_c$ required for the emergence of a zonal jet with meridional wavenumber $n = 1, \ldots, 4$. The eddy field comprises global zonal wavenumbers 1–14. Relevant physical parameters: $\beta = 1.6 \times 10^{-11}$ m^{-1} s^{-1}, Froude number $\lambda^2 = 1$, eddy damping rates $r_2 = 1/5$ day^{-1} and $r_R = 1/15$ day^{-1}, damping rate of the mean $\bar{r}_2 = 1/5$ day^{-1}, and mean cooling $\bar{r}_R$=1/15 day^{-1}. With these parameters instability of the baroclinic jet occurs at $\Delta T_c = 28.3$ K (10^4 km)$^{-1}$.

2007). This stability of the ensemble mean eddy–mean jet equilibrium state depends on the strength of the stochastic excitation $\mathbf{Q}$, the thermal forcing measured by the temperature difference ΔT, the Froude number λ^2, and the dissipation. We primarily examine the stability of equilibrium states as a function of the stochastic excitation $\mathcal{F} = \text{trace}(\mathbf{MQ})/n$ and ΔT.

It can be shown by integration of (27b) in y and imposition of boundary conditions on the eddy motions that the meridional mean of an equilibrium $\mathbf{U}^E$ has the property

$$\int_0^{Ly} U^- \, dy = \int_0^{Ly} U_R^- \, dy, \tag{28}$$

which implies that equilibration cannot result from change in the mean meridional shear or the mean temperature gradient. This is also true of the simulations of Panetta (1993) and Held and Larichev (1996).

For $\Delta T < \Delta T_c$, the radiative equilibrium flow U_R^- is a fixed point of the coupled system (26a) and (26b) for any excitation $\mathcal{F}$ because the ensemble mean eddy fluxes are meridionally constant. For $\Delta T > \Delta T_c$, the radiative equilibrium flow U_R^- is an unstable fixed point of the coupled system (26a) and (26b). We wish to examine the coupled eddy–mean jet stability of these radiative equilibrium fixed points. When $\Delta T < \Delta T_c$, the radiative equilibrium U_R^- becomes unstable only when the stochastic excitation $\mathcal{F}$ exceeds a critical value $\mathcal{F}_c$. When $\Delta T > \Delta T_c$, the radiative equilibrium U_R^- is unstable for all $\mathcal{F}$.

The critical value of stochastic forcing $\mathcal{F}_c$ (mW kg^{-1}) is plotted as a function of ΔT in Fig. 1. Because of the meridional homogeneity of the perturbation equations, the perturbation eigenmodes are harmonic functions. Unstable jet perturbations of harmonic form in the meridional direction emerge when $\mathcal{F}$ exceeds $\mathcal{F}_c$. Figure 1 shows the critical forcings required to destabilize zonal flows with meridional wavenumbers $n = 1, \ldots, 4$.

When the radiative equilibrium is unstable to the formations of jets, the growing zonal jets ultimately equilibrate as finite-amplitude extensions of the unstable eigenmodes of the coupled SSST wave–mean jet system. These equilibria may be stable or unstable fixed points. When unstable, the jets may go to a new stable equilibrium or settle in a limit cycle having periodic

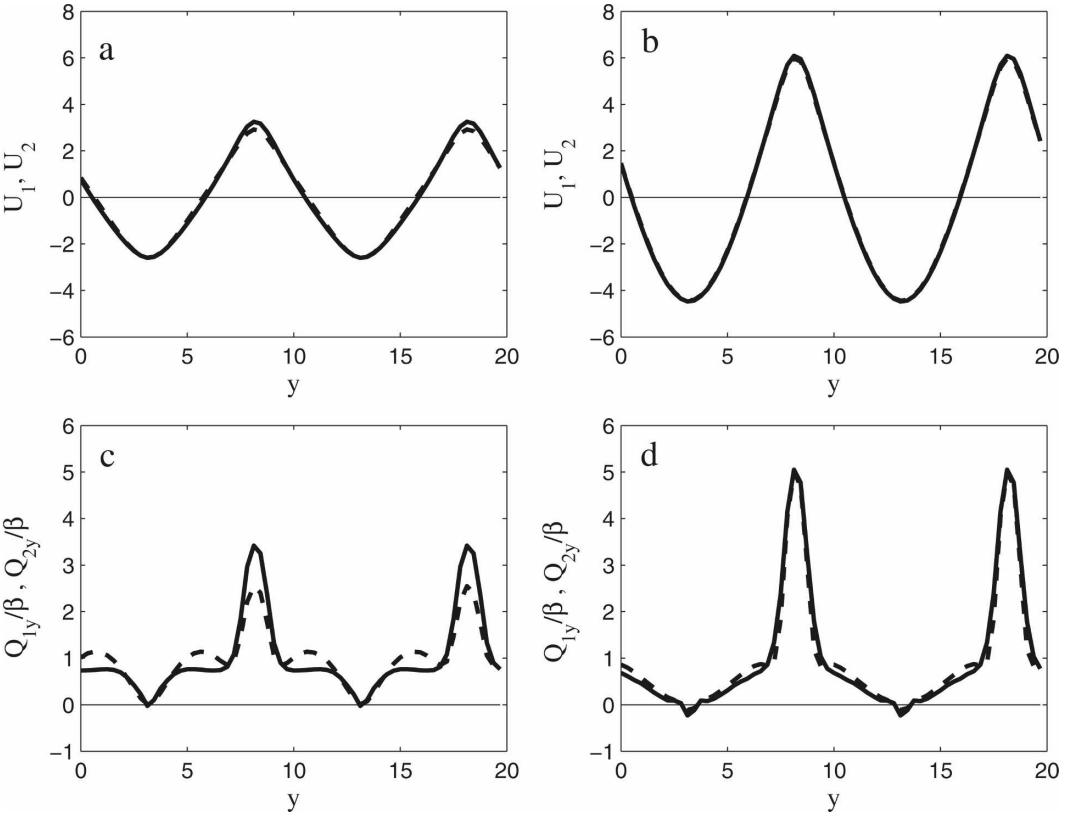

FIG. 2. (a), (b) Meridional structure of the equilibrium upper-layer (continuous line) and lower-layer (dashed line) mean flows maintained by stochastically modeled turbulence in a doubly periodic domain with no mean thermal forcing. Equilibria for two levels of stochastic excitation $\mathcal{F}$ are shown. The stochastic excitation is (a) $\mathcal{F} =$ 5.83 mW kg^{-1} and (b) $\mathcal{F} =$ 58.3 mW kg^{-1} per zonal wavenumber. (c), (d) The corresponding mean potential vorticity gradients of the upper- and lower-layer flows. The nonnormality of the equilibrium flows has increased from 53.9 for the flows in (a) to 155 for the flows in (b). The eddy field comprises global zonal wavenumbers 1–14. The eddy damping parameters are $r_2 =$ 1/5 day^{-1} and $r_R =$ 1/15 day^{-1}; the damping rate of the mean is $\bar{r}_2$=1/5 day^{-1} and the mean cooling is $\bar{r}_R$=1/15 day^{-1}.

behavior; also, chaotic trajectories are possible (Farrell and Ioannou 2003, 2007). However, over a significant parameter range stable fixed points are found, and these are the subject of our study in this paper.

4. Examples of jet equilibria

a. Jet equilibria with no mean thermal forcing

The equilibria found in the absence of mean thermal forcing are, for a wide choice of realistic parameter values, nearly barotropic and similar to those discussed in Farrell and Ioannou (2007), although with appropriate parameter choice and/or vertical asymmetry of stochastic excitation substantial baroclinicity can be maintained.

For sufficiently strong stochastic excitation, multiple equilibria differing in jet meridional wavenumber exist at $\Delta T = 0$ as indicated in Fig. 1.

Examples of meridional wavenumber-2 jet equilibria are shown in Fig. 2 for two values of stochastic excitation. In the first case, the stochastic excitation is $\mathcal{F} =$ 5.8 mW kg^{-1} per wavenumber (Fig. 2a); in the second, the stochastic excitation is $\mathcal{F} =$ 55.8 mW kg^{-1} per wavenumber (Fig. 2b). The first case is stochastically excited with sufficient energy input rate to clearly show departure from the nearly harmonic equilibrium form obtained for slightly supercritical stochastic excitation. The second state is excited at a rate that places the equilibrium state close to the stability boundary just before the bifurcation to meridional wavenumber-1 equilibria as a function of stochastic excitation, and therefore the second equilibrium state departs maximally from the harmonic equilibrium state that results for slightly supercritical stochastic excitation.

In these examples the eddy field comprises 14 zonal wavenumbers. Although the lower layer is Ekman

damped, the equilibria are nearly barotropic and equilibrate close to the Rayleigh–Kuo stability boundary so their meridional spacing scales as $L_\beta = \sqrt{U/\beta}$, and there is pronounced asymmetry between the westward and eastward jets (Farrell and Ioannou 2007). The mean potential vorticity gradient is positive almost everywhere, as shown in Fig. 2. Laboratory experiments using a stratified fluid in a rotating channel with a sloping bottom verify the formation of such stable persistent mean jets when there is no mean thermal forcing (Read et al. 2004, 2007). Although stable, these equilibrated flows are highly nonnormal, with nonnormality increasing[3] from 53.9 to 155 as the stability boundary is approached.

As an example of a nearly barotropic equilibrium, a calculation was done for the Jovian 23°N jet for which accurate velocity data is available (Sánchez-Lavega et al. 2008). Comparison between this accurately observed jet and the corresponding equilibrium obtained using representative Jovian parameters is shown in Fig. 3. Noteworthy are the nearly constant shears and cusplike maximum of the eastward jet and the rounded profile of the westward jet. The physics of these characteristic features of barotropic equilibria in strong turbulence is discussed in detail in Farrell and Ioannou (2007).

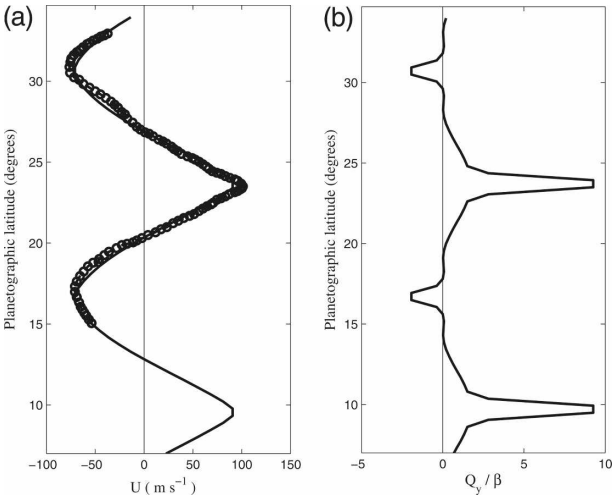

FIG. 3. (a) Simulation of the 23°N jet on Jupiter (solid) compared with observations (circles) adapted from Sánchez-Lavega et al. (2008). The equilibrium jet structure (solid) is barotropic and is barotropically stable. (b) The associated mean vorticity gradient normalized by beta. Parameters are eddy damping $r_{\rm up} = r_{\rm down} = 5.6 \times {\rm s}^{-1}$; mean damping $2.7 \times 10^{-9}\ {\rm s}^{-1}$, as suggested by Conrath et al. (1990) and used by Yamazaki et al. (2004); stochastic forcing 0.34 W m^{-2} per zonal wavenumber in a total Jovian layer depth of 5 bar; and β value corresponding to Jovian planetographic latitude 23°N. The domain is doubly periodic with meridional width equivalent to 28° Jovian latitude. The calculation was performed using the 14 zonal wavenumbers $2\pi n/L_y$, with $n = 1, \ldots, 14$.

b. *Baroclinic jet equilibria with barotropically unstable upper-level jets*

In the absence of mean thermal forcing the equilibria are nearly barotropic. However, when the symmetry between the layers is sufficiently disrupted, baroclinic equilibria can be maintained with strong jets despite the absence of any mean thermal forcing. We find that strong jets satisfying Rayleigh–Kuo necessary conditions for instability form spontaneously as equilibria in the presence of sufficient stochastic excitation and dissipation. As an example, consider the two-layer model with the following parameters: β equal to one-fifth of the terrestrial β, symmetric eddy damping $r_1 = r_2 = 1$ day^{-1}, eddy cooling of $r_R = 1/15$ day^{-1}, and dissipation of the mean $\bar{r}_1 = \bar{r}_2 = 1/250$ day^{-1} with stochastic excitation of only the upper layer at level $\mathcal{F} = 0.972$ mW kg^{-1}. (Throughout this paper, day is abbreviated d.) Equilibrium jet profiles together with the upper and lower layer mean potential vorticity gradients

$$\begin{aligned} Q_{1y} &= \beta - U_1'' + \lambda^2(U_1 - U_2), \\ Q_{2y} &= \beta - U_2'' - \lambda^2(U_1 - U_2), \end{aligned} \tag{29}$$

are shown in Fig. 4. Also shown in the same figure are the barotropic vorticity gradients $\beta - U_i''$ (thick and thin dashed lines). This stable equilibrium jet is baroclinic, with the upper-level flow violating Rayleigh–Kuo stability condition by 10β.

c. *Jet equilibria with mean thermal forcing*

Consider a stochastically excited baroclinic flow with mean thermal forcing. As the mean thermal forcing is increased, jets equilibrate that are marginally stable and highly nonnormal. Examples of such baroclinically adjusted jets are shown in Fig. 5a for two different levels of stochastic excitation, $\mathcal{F} = 0.48$ mW kg^{-1} and $\mathcal{F} = 1.34$ mW kg^{-1}, with mean thermal forcing $\Delta T = 30$ K$(10^4{\rm km})^{-1}$ [recall that the stability boundary is $\Delta T_c = 28.3$K $(10^4{\rm km})^{-1}$]; this figure shows meridional wavenumber-3 jet equilibria. The second equilibrium in Fig. 5b is close to the structural stability boundary just before the bifurcation to meridional wavenumber-2 equilibria as a function of forcing. Note that both equilibria have a mean supercriticality parameter $\xi = 8U_R^-/(\beta\lambda^2) = 2.15$. The equilibrated flows in Fig. 5 and most of the

[3] The measure of nonnormality we use is the ratio of the variance maintained by stochastic excitation of this system to the variance maintained in the equivalent normal system that has the same eigenvalues but orthogonal eigenvectors when both are forced with identical stochastic excitation $\mathbf{Q} = \mathbf{I}$ (Ioannou 1995; Farrell and Ioannou 1996).

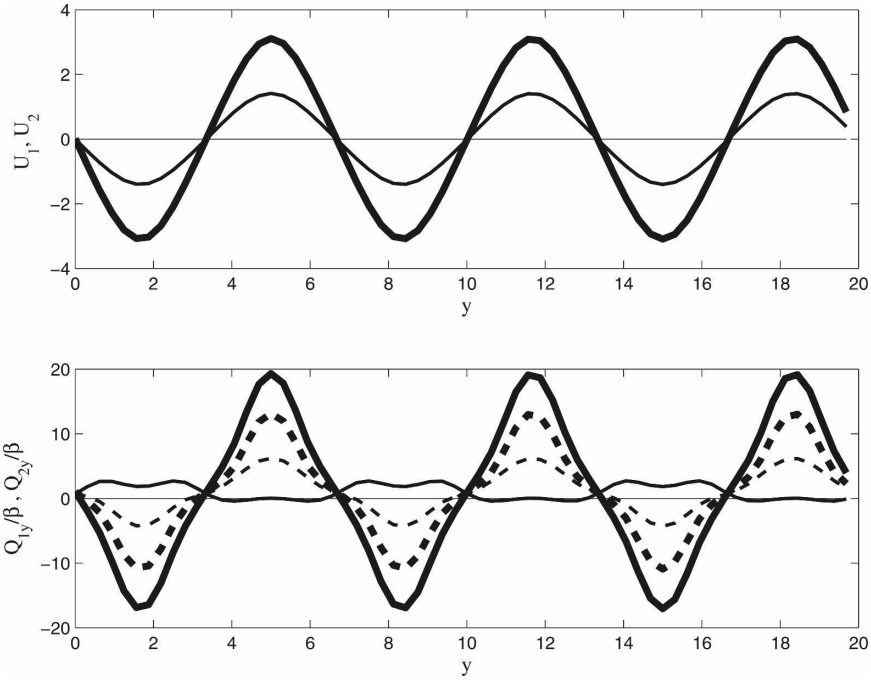

FIG. 4. (top) Meridional structure of the equilibrium upper-layer (thick line) and lower-layer (thin line) mean flows maintained by stochastically modeled turbulence in a doubly periodic domain with no mean thermal forcing. The equilibrated flows violate the Rayleigh–Kuo barotropic stability condition but the flows are stable. The layers are equally damped at rate $r_1 = r_2 = 1$ day^{-1}, the eddy cooling rate is $r_R = 1/15$ day^{-1}, and the dissipation of the mean occurs at rate $\bar{r}_1 = \bar{r}_2 = 1/250$ day^{-1}. Stochastic excitation of only the upper layer at level $\mathcal{F} = 0.972$ mW kg^{-1} is used. The other parameters are $\lambda^2 = 1$ and $\beta = 1/5$ of the terrestrial value in order to simulate Jovian conditions. (bottom) The corresponding mean potential vorticity gradients measured in units of β of the upper-layer (solid thick line) and lower-layer (dashed thick line) flows. Also shown are the corresponding barotropic potential vorticity gradients (solid and dashed lines, respectively).

examples shown in this paper have mean supercriticality $\xi > 1$ and yet are manifestly stable.

The equilibrated eastward jets can be highly baroclinic because baroclinicity of the eastward jet increases the already positive potential vorticity gradient—unlike the case of the westward jets, for which the baroclinic shear is suppressed at equilibrium to preserve stability, as can be seen in Figs. 5c,d. The presence of dissipation allows the potential vorticity gradient of the equilibrated jets to change sign, substantially violating the Charney–Stern stability condition, while retaining stability. These baroclinically adjusted states are primarily equilibrated by meridional confinement interacting with dissipation (Ioannou and Lindzen 1986; James 1987; Roe and Lindzen 1996).

d. Mechanism controlling turbulent heat flux

Regulation of the mean heat flux in a doubly periodic two-layer baroclinic turbulence model has been the subject of much study (Haidvogel and Held 1980; Panetta and Held 1988; Held and Larichev 1996; Pavan and Held 1996; Lapeyre and Held 2003). We investigate the role of emergent jets in this process by modeling a turbulent supercritical flow in which equilibrated jets have enforced stability.

To address the role of multiple jets (each of which has been baroclinically adjusted to be near a stability boundary) in regulating the heat flux across a wide channel, we perform an experiment in which a supercritical radiative equilibrium constant shear state is perturbed by a small random initial jet structure and allowed to equilibrate with zero initial eddy covariance. The temperature difference of the radiative equilibrium is 35 K over a distance of 10^4 km, corresponding to a supercriticality of $\xi = 2.51$. The equilibration occurs in a characteristic progression in which the eddy field grows rapidly to reach a high overshoot eddy variance and heat flux, at which time the eddy field organizes jets that grow and ultimately equilibrate the combined eddy

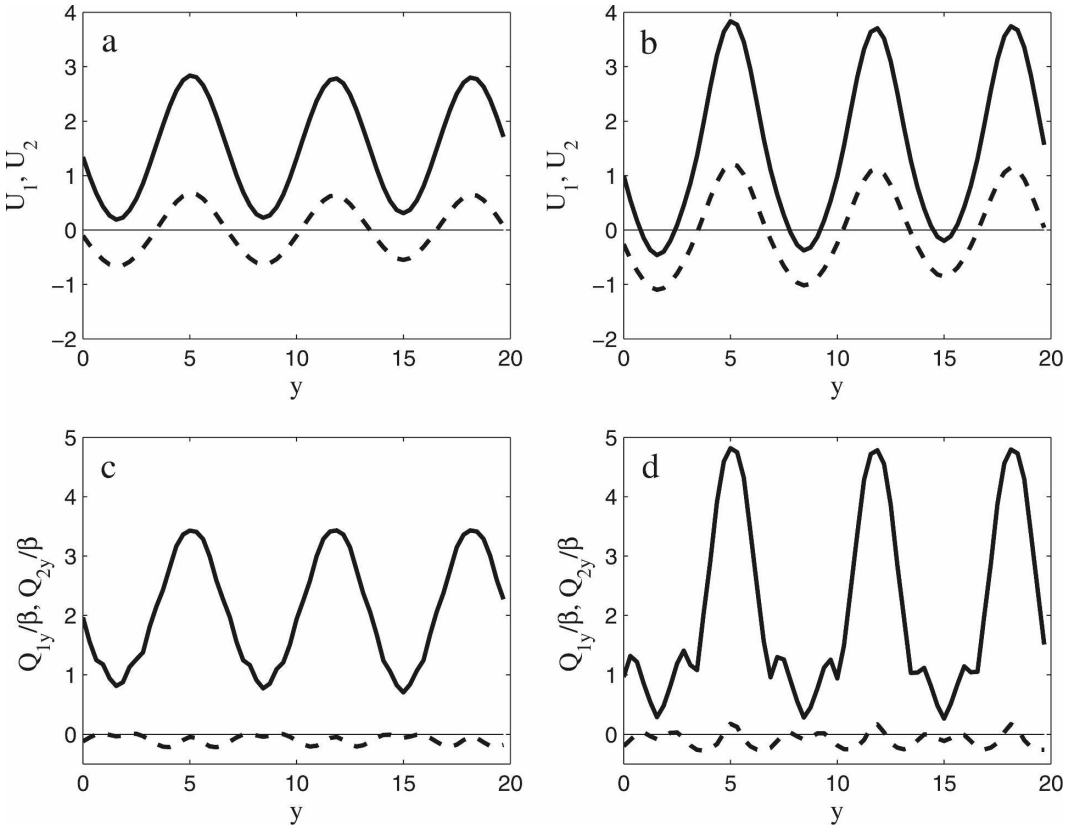

FIG. 5. (a), (b) Meridional structure of the equilibrium upper-layer (continuous line) and lower-layer (dashed line) mean flows maintained by stochastically modeled turbulence in a doubly periodic domain with mean thermal forcing $\Delta T = 30$ K $(10^4$ km$)^{-1}$. Equilibria for two levels of stochastic excitation $\mathcal{F}$ are shown: (a) $\mathcal{F} = 0.48$ mW kg^{-1} and (b) $\mathcal{F} = 1.34$ mW kg^{-1} per zonal wavenumber. (c), (d) The corresponding mean potential vorticity gradients of the upper- and lower-layer flows. Both equilibrium flows are supercritical with the same supercriticality parameter $\xi = 2.18$ but are exponentially stable because of the meridional variation of the flows and the dissipation. The nonnormality of the equilibrium flows has increased from (a) 26.7 to (b) 53. The eddy field comprises global zonal wavenumbers 1–14. The eddy damping parameters are $r_2 = 1/5$ day^{-1}, $r_R = 1/15$ day^{-1}, and $r_{\text{eff}} = 1/20$ day^{-1}. The damping rate of the mean is $\bar{r}_2 = 1/5$ day^{-1}; the mean cooling rate is $\bar{r}_R = 1/15$ day^{-1}.

and mean jet system at a lower equilibrium total eddy energy. The time development of the flow and the associated fluxes are shown in Figs. 6 and 7. This progression is commonly observed when an eddy–mean jet system is established or perturbed (Panetta and Held 1988; Panetta 1993; Chen et al. 2007). To better understand control of the heat flux by the jets, an experiment was performed in which for the first 60 days the coefficient of Newtonian cooling of the mean baroclinic flow was set to $\bar{r}_R = 1/3$ day^{-1} before being switched to $\bar{r}_R = 1/15$ day^{-1} at day 60. By $t = 60$ the flow has been stabilized (Fig. 7c) and both the jets and the eddies have equilibrated as indicated by the constant value of the maximum wind in layer 1 and the maximum shear shown in Fig. 7a, the latitudinally averaged heat flux in Fig. 7b, and the latitudinally averaged total eddy energy in Fig. 7d. Under strong mean thermal relaxation the jets are suppressed, and as a result the eddy equilibrium kinetic energy and the eddy heat flux decrease when the relaxation is decreased to $\bar{r}_R = 1/15$ day^{-1} at $t = 60$ day, allowing the jet to increase in amplitude, which increases jet stability. This behavior is analogous to the midwinter suppression of eddy variance that is observed in the Pacific storm track in winter (Nakamura 1992; Zhang and Held 1999), a phenomenon that has also been simulated for conditions during the last glacial maximum (Li and Battisti 2008). The common thread in the two-layer model simulation and the observations is that the westerlies become sharper and stronger while the eddy activity is reduced. The time development of the fluxes and variances show that at first both the mean flow and the eddy fluxes and variances overshoot their equilibrium values before jets develop, which then suppress both the eddy heat flux and the variance, demonstrating the crucial role of the jets in controlling the mean equilibrium state. We conclude

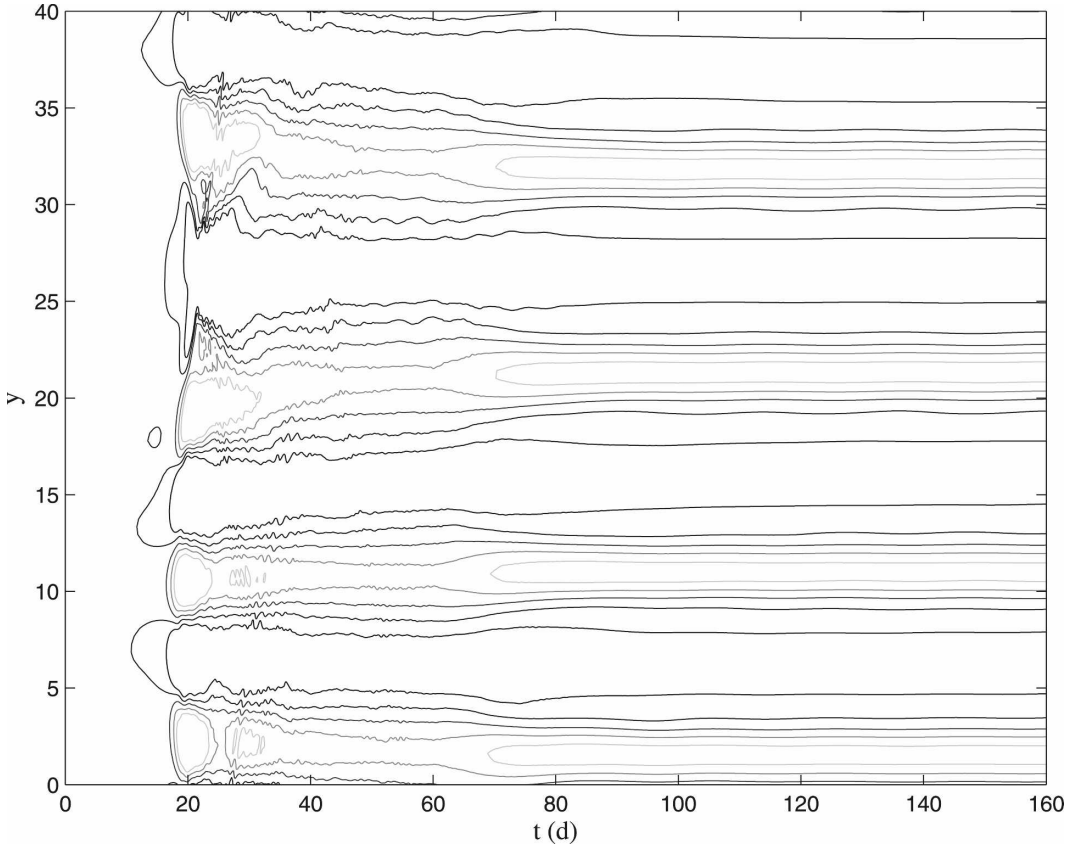

FIG. 6. Contours of the zonal mean velocity in the upper layer as a function of time and meridional distance. The flow starts at $t = 0$ with a random perturbation about the radiative equilibrium uniform flow that maintains a temperature difference of 35° K $(10^4 \text{ km})^{-1}$. The eddy field comprises global zonal wavenumbers 1–14. The eddy damping parameters are $r_2 = 1/5 \text{ day}^{-1}$, $r_R = 1/15 \text{ day}^{-1}$, $r_{\text{eff}} = 1/20 \text{ day}^{-1}$. The damping rate of the mean is $\bar{r}_2 = 1/5 \text{ day}^{-1}$; the mean cooling rate is $\bar{r}_R = 1/3 \text{ day}^{-1}$ for the first 60 days and then changes to $\bar{r}_R = 1/15 \text{ day}^{-1}$ at $t = 60$ days. The stochastic excitation is $\mathcal{F} = 0.48 \text{ mW kg}^{-1}$ per zonal wavenumber.

that regions containing a number of jets baroclinically equilibrate each individual jet while the mean shear remains supecritical and that this baroclinic equilibration of the individual jets then determines the equilibrium heat flux.

5. Scaling, baroclinic adjustment, and the role of nonnormality

Equilibrium jets that form in strong turbulence are adjusted to marginal stability. Although stable, these highly sheared flows are also highly nonnormal, supporting large transient perturbation amplification. One consequence of this stability and nonnormality in the earth's midlatitude atmosphere is the association of cyclone formation with the chance occurrence in the turbulence of optimal or near-optimal initial conditions (Farrell 1982, 1989; Farrell and Ioannou 1993c; DelSole 2004a, 2007). These optimal perturbations are analogous to the dangerous inputs that render feedback-stabilized mechanical and electronic systems fragile (Zhou and Doyle 1998), and it is excitation of these amplifying perturbations by the nonlinear wave–wave interactions, here parameterized by stochastic excitation, that maintains the turbulent variance (Farrell and Ioannou 1993c,d; DelSole 2007).

In addition to explaining the stability, high nonnormality, and the centrality of transient growth in jet dynamics, we argue that these equilibria provide an explanation for the scaling laws of fluxes as a function of parameters influencing jet stability found in baroclinic turbulence simulations (Zhou and Stone 1993; Held and Larichev 1996; Barry et al. 2002; Zurita-Gotor 2007).

To introduce this last idea, consider the linear dynamics of streamwise rolls in an unbounded shear flow with rotation in the spanwise direction. This system is governed by the Reynolds matrix, which provides a

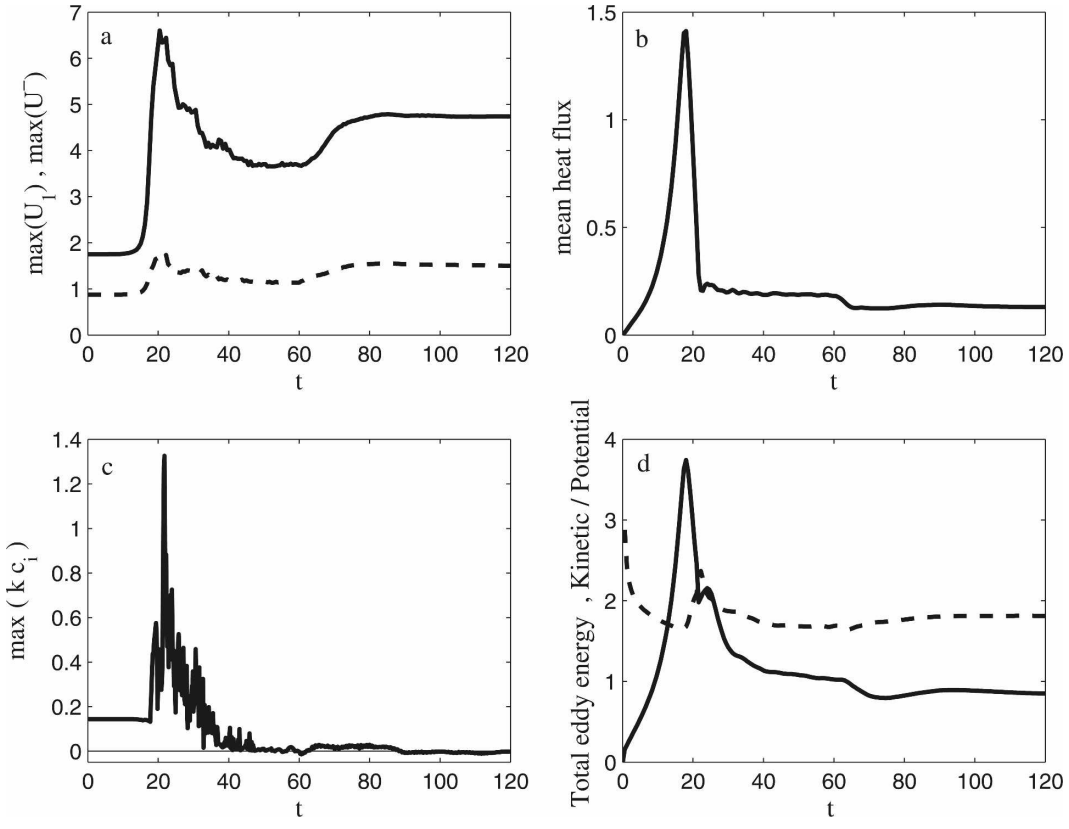

FIG. 7. (a) Nondimensional maximum upper-level velocity (solid) and maximum shear (dashed line) as a function of time (unit velocity is 11 m s^{-1}). (b) Mean heat flux as a function of time. (c) Maximum growth rate of the instantaneous flow as a function of time (day^{-1}). (d) Total eddy energy (solid) and ratio of eddy barotropic to eddy baroclinic energy (dashed) as a function of time. The parameters are as in Fig. 6.

convenient example of a dynamical system in which stability and nonnormality interact:

$$\mathbf{A} = \begin{bmatrix} -\nu(l^2 + m^2) & -(\alpha - 2\Omega) \\ -2\Omega l^2/(l^2 + m^2) & -\nu(l^2 + m^2) \end{bmatrix}. \quad (30)$$

In (30), Ω is a rotation rate, α the constant shear of the mean flow, ν the coefficient of viscosity, l the spanwise wavenumber, and m the vertical wavenumber (see appendix). With $\Omega = 0$, this matrix models the dynamical system of a streamwise roll perturbation in an unbounded constant shear boundary layer (Farrell and Ioannou 1993a). In addition, with $\Omega = 0$ this dynamical system is stable, with decay rate $-\nu(l^2 + m^2)$, but with nonnormality increasing with α, so that it supports optimal transient growth increasing proportional to α^2 and occurring at time $[\nu(l^2 + m^2)]^{-1}$, implying that the variance grows proportional to α^2 for constant viscosity. With the modification of including a spanwise oriented rotation rate Ω, the decay of the least damped mode also decreases as α increases so that when $\alpha_c = 2\Omega + \nu^2(l^2 + m^2)^3/(2\Omega l^2)$, the matrix becomes unstable. The rotation rate Ω destabilizes the Reynolds matrix by coupling the streamwise and spanwise velocity components. With this addition, the Reynolds matrix provides a versatile model of the interplay between stability and nonnormality in the vicinity of a stability boundary such as that to which the coupled eddy–mean jet system generally adjusts jets. We now use this matrix to understand how power-law behavior arises in strongly turbulent equilibria such as the midlatitude jet. When α is increased in the Reynolds system and the dynamical matrix $\mathbf{A}$ is forced with constant-variance white noise in each variable, the variance increases proportional to α^2. In contrast, the variance in the equivalent normal system, in which the change in the eigenvalues is retained but the eigenvectors are assumed orthogonal, exhibits no power-law behavior but only the familiar resonance-induced $(\alpha - \alpha_c)^{-1}$ divergence in the immediate neighborhood of the stability boundary as shown in Fig. 8. The momentum flux also increases proportional to α, deviating from this power only in the immediate neighborhood of the critical shear.

Power-law behavior is similarly generic in strongly

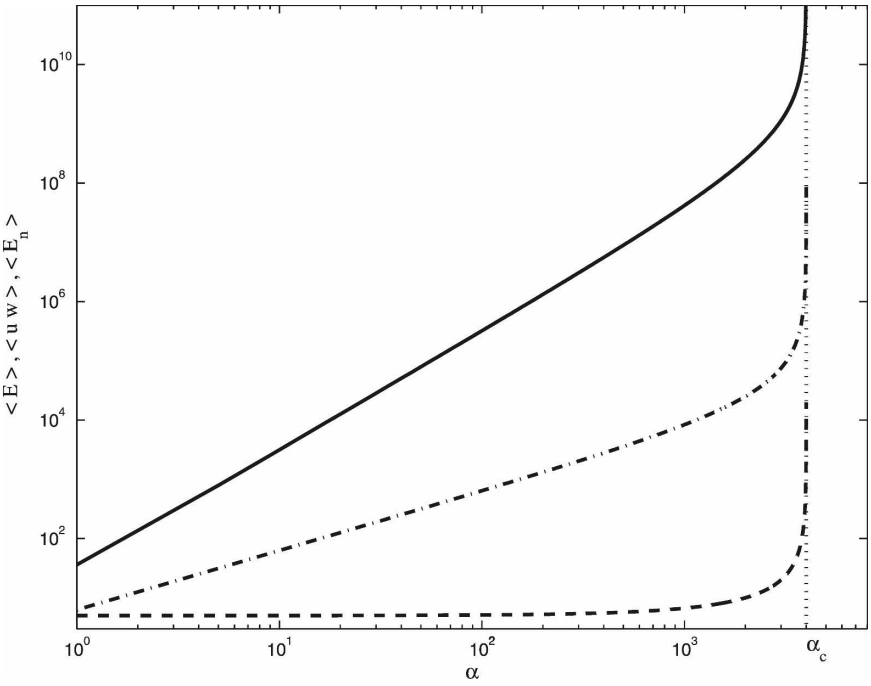

FIG. 8. For the Reynolds example system: the ensemble mean energy $\langle E \rangle$ as a function of the shear α for rotation rate $\Omega = 10^{-5}$, $\nu = 0.1$ and perturbation wavenumbers $l = m = 1$. The critical shear at which the matrix becomes unstable is $\alpha_c = 4000$. The variance increases as α^2, deviating from this power law behavior only for shears very close to α_c. The dashed–dotted curve shows the momentum flux $\langle \overline{uw} \rangle$, which can be seen to vary as α. The dashed curve shows the variance $\langle E_n \rangle$ maintained by the equivalent normal system with the same decay rate as **A**; this variance is almost constant, increasing only for shears close to α_c.

turbulent jet equilibria, but the specific power depends on the stability parameter involved, the variable, and the growth mechanism. The origin of power-law scaling behavior can be understood by considering the growth of optimal perturbations, which dominate the maintenance of variance in highly nonnormal systems. Figure 9 shows the increase of the mean baroclinic and barotropic energy generation rates

$$P_{\text{em}} = \int_0^1 -2\lambda^2 U^- \left\langle \overline{\psi_x^+ \psi^-} \right\rangle dy \quad \text{and} \tag{31a}$$

$$K_{\text{em}} = \int_0^1 \left[U^+ \left(\left\langle \overline{\psi_x^+ \psi_{yy}^+} + \overline{\psi_x^- \psi_{yy}^-} \right\rangle \right) + U^- \left(\left\langle \overline{\psi_x^+ \psi_{yy}^-} + \overline{\psi_x^- \psi_{yy}^+} \right\rangle \right) \right] dy, \tag{31b}$$

and of the quantity

$$\overline{vT} = \left\langle \overline{\psi_x^+ \psi_{yy}^-} + \overline{\psi_x^- \psi_{yy}^+} \right\rangle, \tag{32}$$

which is proportional to the heat flux, with criticality of the equilibrated flow evaluated at the jet maxima $\xi = 4(U_1 - U_2)/(\beta\lambda^2)$. The energy generation rates increase as ξ^4 in agreement with simulations showing power-law scaling of the flux–gradient relationship, which has been interpreted as higher-order thermal diffusion with diffusivity increasing as the third power of the temperature gradient (Held and Larichev 1996; Zurita-Gotor 2007). The heat flux (at the center of the jet and its mean value) increase with criticality as ξ^3. At high criticality, departures from the power-law behavior shown in Fig. 10 result if the meridional average shear is used to calculate the criticality rather than the shear at the jet axis. The reason is that the shear becomes meridionally concentrated at high criticality. Figure 10 also shows the heat flux as a function of the criticality taken as the meridional average shear.

6. Quantization and abrupt jet reorganization

As stochastic excitation is increased or mean shear is increased or static stability decreased, equilibrium jets strengthen and adjust in structure to maintain a stable equilibrium. However, if the jet number is quantized, as is the case for the earth, eventually no stable jet equilibrium is possible at the extant wavenumber and the eddy–mean jet system undergoes a bifurcation in which

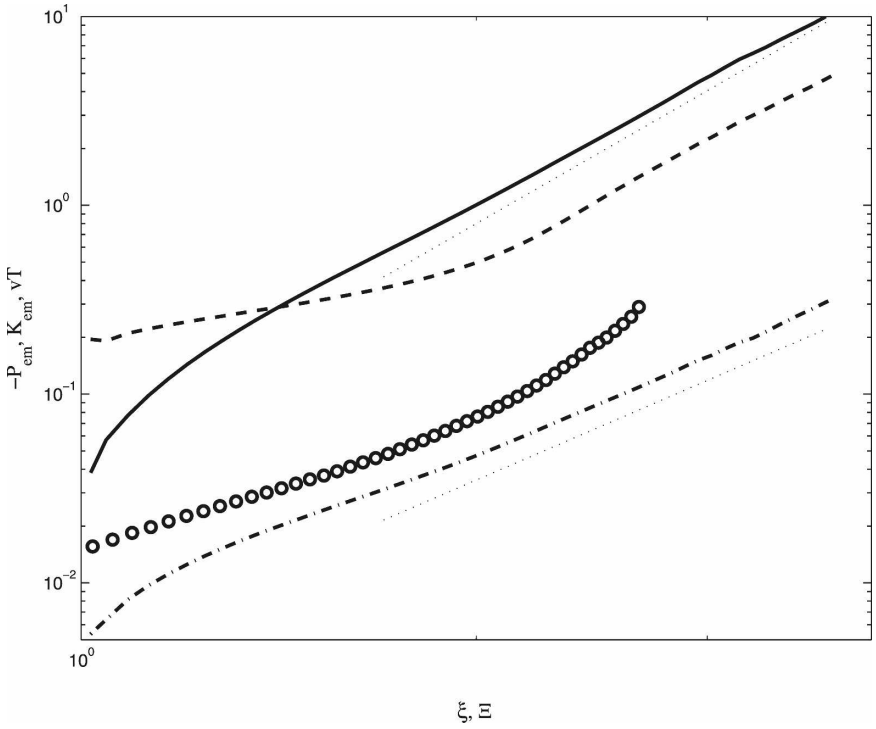

FIG. 9. The mean eddy baroclinic energy generation rate $-P_{\mathrm{em}}$ (solid line), the mean eddy barotropic energy generation rate K_{em} (dashed line), and the heat flux $\overline{vT}$ at the center of the jet (dashed–dotted line) as a function of the criticality parameter $\xi = [4(U_1 - U_2)/\beta L_2]$ evaluated at the jet maximum, together with the mean heat flux as a function of the mean criticality Ξ (circles). The eddy generation rates increase as ξ^4 (indicated with the upper dotted line) and the heat flux increases as ξ^3 (indicated with the lower dotted line).The mean heat flux also has the same power-law behavior. The heat flux does not scale with the mean criticality Ξ because as criticality increases it becomes increasingly localized near the jet center. The stochastic excitation is $\mathcal{F} = 0.24$ mW kg^{-1} per mode. The eddy field comprises global zonal wavenumbers 1–14. The eddy damping parameters are $r_2 = 1/5$ day^{-1}, $r_R = 1/15$ day^{-1}, and $r_{\mathrm{eff}} = 1/20$ day^{-1}; the damping rate of the mean is $\bar{r}_2 = 1/5$ day^{-1}; the mean cooling rate is $r_R = 1/15$ day^{-1}.

a new equilibrium is established, typically at the next lowest allowed wavenumber. This reorganization occurs abruptly as a parameter-controlling jet amplitude is changed. Similar behavior has been observed to occur in model systems (Lee 1997, 2005; Robinson 2006) and has been inferred to occur in the climate record (Fuhrer et al. 1999; Wunsch 2003; Alley et al. 1993). It provides a mechanism for producing abrupt changes in climate statistics by changing the source region of climate markers such as isotopes that are recorded in ice cores (Wunsch 2003). More fundamentally, because the axis of the polar jet is also an axis of concentration of surface stress, the abrupt displacement of the polar jet could change the climate itself by influencing the ventilation rate of the intermediate depths in the ocean (Toggweiler et al. 2006).

A parameter of the baroclinic system that may vary with climate change is the static stability; in a warmer world, troposphere static stability is expected to increase as a result of decrease in the saturated adiabatic lapse rate. This effect is generally accepted for the tropics and subtropics (Held 1982; Sarachik 1985; Xu and Emanuel 1989), and although the extent of the increase in the extratropics is less well established, it is expected to also apply in midlatitudes (Juckes 2000; Frierson 2006). The opposite tendency is expected to have characterized ice age climates.

The growth rate and structure of baroclinic waves are strongly influenced by static stability, with the growth rate and the penetration depth scaling inversely with the buoyancy frequency (Vallis 2006), so that it is of interest to add static stability to stochastic excitation and thermal gradient as parameters in our analysis.

Lower static stability implies a higher Froude number as $\lambda^2 = (fL)^2/(NH)^2$. We find that static stability serves as a bifurcation parameter analogous to the

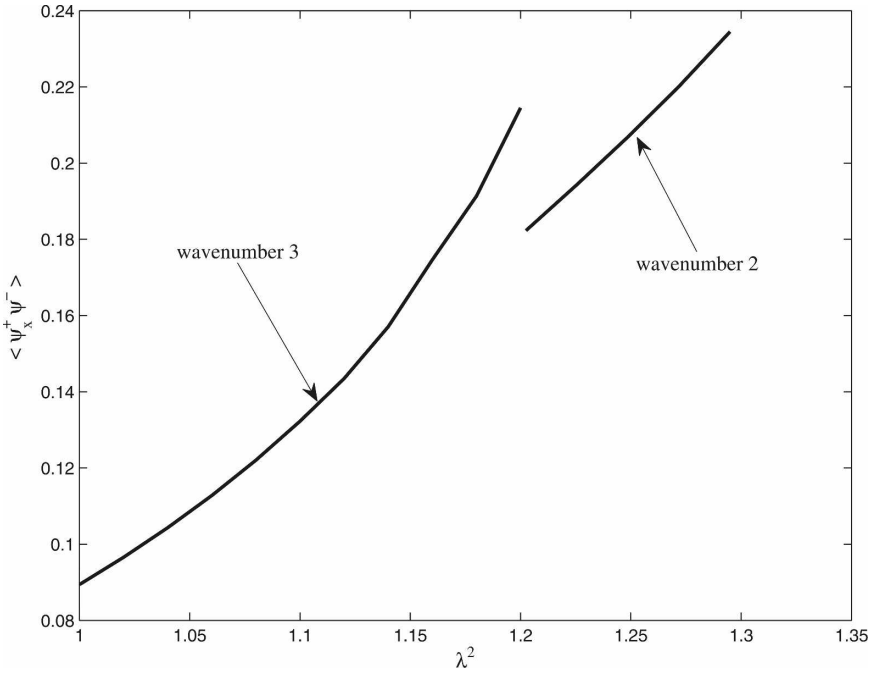

FIG. 10. For the equilibrium jets, the maximum heat flux $\langle \overline{\psi_x^+ \psi^-} \rangle$ as a function of Froude number λ^2. At $\lambda^2 = 1.2$ there is an abrupt transition from a meridional wavenumber-3 jet to a meridional wavenumber-2 jet. The thermal forcing is $\Delta T = 30$ K $(10^4 \text{ km})^{-1}$ and the stochastic excitation is $\mathcal{F} = 0.49$ mW kg^{-1} per mode. The eddy field comprises global zonal wavenumbers 1–14. The eddy damping parameters are $r_2 = 1/5$ day^{-1}, $r_R = 1/15$ day^{-1}, and $r_{\text{eff}} = 1/20$ day^{-1}; the damping rate of the mean is $\bar{r}_2 = 1/5$ day^{-1}; the mean cooling rate is $\bar{r}_R = 1/15$ day^{-1}.

mean shear in its influence on jet equilibria and that small changes in static stability can induce abrupt reorganization of jet equilibria as shown in Fig. 10. In this example, bifurcation from a wavenumber-3 to a wavenumber-2 jet occurs as shown in Fig. 11. At $\lambda^2 = 1.2$, there is an abrupt transition from a meridional wavenumber-3 jet to a meridional wavenumber-2 jet for thermal forcing $\Delta T = 30$ K $(10^4 \text{ km})^{-1}$ and stochastic excitation of $\mathcal{F} = 0.49$ mW kg^{-1} per mode.

7. Discussion

a. Relation between SSST equilibria and the barotropic governor

It was noticed by James (1987) that baroclinic jets in GCM simulations tend to equilibrate by modifying the barotropic shear and that substantially greater baroclinic shear can be maintained in these horizontally sheared flows than would be compatible with stability in a horizontally homogeneous flow. This phenomenon, called the barotropic governor, was confirmed by stability analyses, and it implies that the baroclinic adjustment process is in part independent of changes in vertical shear (Lindzen 1993). The ensemble mean eddy–mean jet equilibria provide insight into the mechanism underlying the barotropic governor by showing that a barotropic governor stabilized state is an attracting equilibrium state of the ensemble mean eddy–jet coupled system. This mechanism of stabilization by confinement due to horizontal shear, which we have seen in the two-layer model, was analyzed by Ioannou and Lindzen (1986) and Roe and Lindzen (1996).

b. Relation between SSST equilibria and baroclinic adjustment

Baroclinic adjustment was originally invoked to explain the observed near-baroclinic neutrality of the midlatitude jets (Stone 1978; Stone and Miller 1980). This adjustment to marginal stability has been confirmed in observed flows (Hall and Sardeshmukh 1998; Sardeshmukh and Sura 2007) and in two-layer model turbulence (Cehelsky and Tung 1991; DelSole and Farrell 1996; Roe and Lindzen 1996). Baroclinic adjustment is important as a concept because of the insight it offers into the nature of baroclinic turbulence. It is also important as the theoretical underpinning for the con-

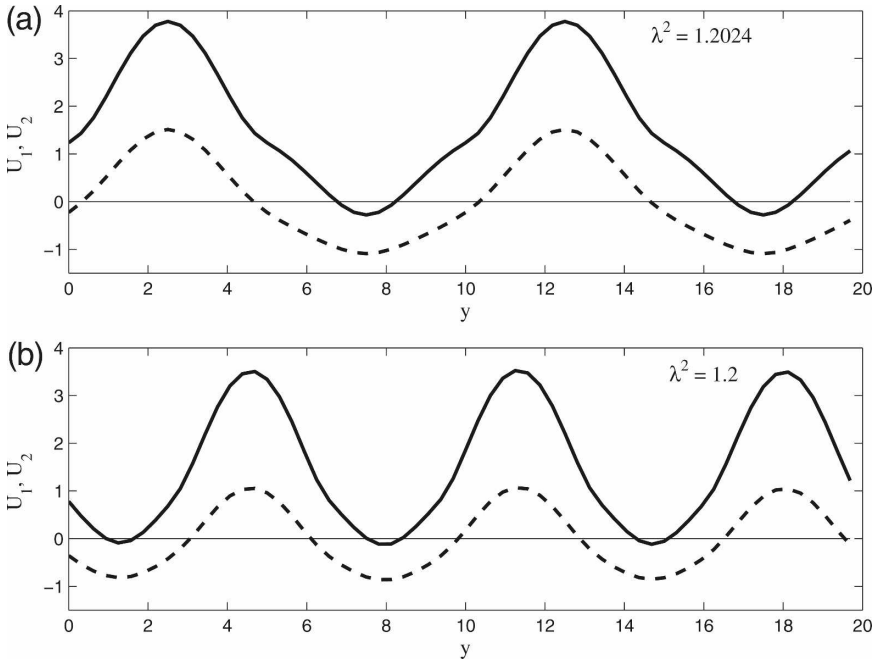

FIG. 11. Structure of the equilibrium upper-layer (continuous line) and lower-layer (dashed line) mean flows maintained in a doubly periodic domain with mean thermal forcing $\Delta T = 30$ K $(10^4 \text{ km})^{-1}$ and stochastic excitation of $\mathcal{F} = 0.49$ mW kg^{-1} per mode. (a) The meridional wavenumber-2 jet that bifurcates from (b) the meridional wavenumber-3 jet. The parameters are as in Fig. 11.

cept of compensation, which has implications for climate dynamics. The idea of baroclinic compensation is that because baroclinic turbulence maintains a relatively constant temperature gradient in mid and high latitudes, the influence of any change in alternative heat transport mechanisms such as ocean heat transport is diminished: the baroclinic transport adjusts up or down to compensate for any variation in these transport mechanisms so their variation cannot substantially change the climate. Baroclinic adjustment has been extensively studied and two main ideas have emerged: (i) adjustment due to modal instabilities themselves producing the heat flux when the stability boundary is crossed, with these modal instabilities then adjusting the system to a stability boundary (Stone 1978; Cehelsky and Tung 1991; Gutowski et al. 1989; Lindzen and Farrell 1980; Lindzen 1993); and (ii) high-order turbulent diffusion due to baroclinic eddies producing rapid increase in heat transport coincident with but not causally related to unstable growth itself (Pavan and Held 1996; Held and Larichev 1996). We have seen that ensemble mean eddy–mean jet equilibria approach a stability boundary when the turbulence is sufficiently strong; thus, these equilibria provide a natural interpretation for the phenomenon of baroclinic adjustment. This interpretation unites the previous interpretations in the following sense: the stability boundary is important but not, as in the original baroclinic adjustment interpretations, because growth occurs when this boundary is exceeded; rather, it is because turbulent fluxes produced by the nonnormal interaction among a larger set of waves increase rapidly as the stability boundary is approached, thereby producing equilibrium states of the coupled mean flow–turbulence system that occur near stability boundaries when the turbulence is strong. Turbulent transport is important because it is the spectrum of waves, not just the instabilities, that produces the transport; however, the equilibrium flux–gradient relationship cannot be understood from homogeneous turbulence closure arguments because the transport at equilibrium is essentially controlled by the inhomogeneity of the equilibrium states and particularly by the organization of the mean flow into jets. Although a baroclinically adjusted state can result from a wide variety of jet structure modifications (including reduction in the temperature gradient and meridional confinement), an advantage of the ensemble eddy–mean jet equilibria calculation we have done is that it provides a prediction of the particular structure changes involved in producing the baroclinically equilibrated state so that it is a predictive and not simply a diagnostic theory for jet equilibria.

8. Conclusions

Large-scale zonal jets emerge spontaneously from baroclinic turbulence in the absence of jet-scale forcing; examples include the Jovian banded winds and the earth's polar-front jet. The primary physical mechanism maintaining these jets is turbulent eddy fluxes that have been systematically organized by the jet to support the jet structure. This phenomenon arises from an ubiquitous instability of turbulent fluids to jet formation, which occurs because turbulent eddies are always available to be organized by an appropriately configured perturbation zonal jet to produce a flux proportional to jet amplitude. Because this local upgradient flux is proportional to jet amplitude, it results at first in an exponential jet growth rate. This is a new mechanism for destabilizing turbulent flows that is essentially emergent from the interaction between the mean state and its turbulence. In this work, we have provided a detailed dynamical explanation for the systematic mutual organization of the jet and the turbulent eddy fluxes required to produce this instability. A key ingredient of this theory is stochastic turbulence modeling, which provides an analytic solution for the eddy covariance in statistical equilibrium with the jet so that the feedback between the jet and the turbulence can be analyzed in detail. The primary analytical tool of SSST is the coupled dynamical system consisting of the evolution equation for the eddy fluxes obtained from a statistical equilibrium stochastic turbulence model together with the evolution equation for the zonal jet. This nonlinear coupled set of equations exhibits robust and relatively simple behavior. Using this model, we find that the state of thermal wind balance with a constant temperature gradient on a doubly periodic beta plane is a stationary state of the coupled system for baroclinically stable shear; however, this stationary state is exponentially unstable to zonal jet perturbations if the turbulence is sufficiently strong, and these zonal perturbations evolve into jets that grow and adjust in structure until reaching finite-amplitude equilibrium. If a baroclinically unstable mean shear is thermally forced, then the equilibration is again a function of both the thermal gradient and the stochastic excitation, and equilibria are also found.

With weak excitation, the equilibrated jets are sinusoidal and nearly barotropic. There may be a number of unstable meridional jet wavenumbers each leading to an equilibrated state. When evolved from an unbiased initial condition, the wavenumber of a weakly forced jet is that of the most unstable eigenmode of the linearized SSST system, and the amplitude at equilibrium results from the balance between the weakly nonlinearly modified upgradient eddy momentum flux and dissipation. But as the stochastic excitation (or another stability-related parameter such as the static stability) changes so as to tend to destabilize the jet, its structure evolves in a characteristic progression that contrives to maintain the jet equilibria near a modal eddy stability boundary despite the increase in jet amplitude. The eastward jet contracts and becomes increasingly baroclinic, whereas the westward jet expands, maintaining less baroclinicity. Contraction of meridional scale in the eastward jet augments the effective beta, as does an arbitrary vertical shear, so the eastward jet shear may become quite large. This mechanism for stabilizing the baroclinic mode in eastward shear may be viewed as a manifestation of the barotropic governor (Ioannou and Lindzen 1986; James 1987; Lindzen 1993). No such stabilization of the westward jet is possible, so the vertical shear remains small in the westward jet to prevent baroclinic eddy mode destabilization while the meridional scale expands to approach the Rayleigh–Kuo condition for barotropic modal stability. Consequently, the equilibrium jet structure exhibits pronounced asymmetry, with the eastward jet being sharper than the westward jet; and of the three space scales in the jet structure problem, the beta scale $L_\beta=\sqrt{U_{\max}/\beta}$ emerges as the primary meridional structure scale.

Dissipation and quantization of both meridional and zonal wavenumbers often results in stable states that in some degree satisfy either or both of the Charney–Stern and Rayleigh–Kuo conditions. This is no contradiction because these conditions are necessary and not sufficient conditions and in any case apply strictly only to flows without dissipation. It is important to keep in mind that the fact that an observed jet satisfies one or both of these necessary conditions need not imply that the jet is unstable.

Adjustment of jets to marginal stability can take place in many ways, including reducing the vertical shear, increasing the horizontal shear, and, in the primitive equations, modifying the static stability. Because all of these mechanisms are available, the mere knowledge that the system is adjusted to a state of marginal stability, although useful as a diagnostic, does not constitute a predictive theory for jet structure. A particular advantage of the SSST is that it transcends this ambiguity by the crucial additional requirement of equilibrium between the turbulent fluxes and the jet, which identifies in the space of all marginal equilibria the consistent and therefore the physically relevant one.

Adjustment to stable but highly amplifying states with power-law behavior for flux–gradient relations is characteristic of jet equilibria. Analogous behavior of-

ten arises when a feedback controller is imposed to stabilize a multidimensional unstable mechanical or electronic system (Zhou and Doyle 1998). We have shown that the state of high nonnormality together with marginal stability is inherent because turbulence maintains flow stability with a naturally occurring feedback controller.

In the presence of meridional quantization, such as that enforced by finite planetary radius, an abrupt reorganization of jet structure occurs as stochastic forcing or another parameter controlling jet amplitude increases. This reorganization occurs as the increasing westward jet amplitude forces an incipient instability for the particular dissipation and spatial confinement of the model. At this point, the jet reorganizes to the next lower allowed meridional wavenumber and the process continues.

This abrupt reorganization of jet structure as a function of parameter change is an example of a fundamental process in jet dynamics with important climate connections. Discontinuous reorganization of eddy-driven jets can alter both climate statistics (Fuhrer et al. 1999; Wunsch 2003) and the climate itself (Toggweiler et al. 2006). Abrupt change of climate and climate statistics is common in the climate record (Alley et al. 1993), but mechanisms for producing abrupt transitions have been difficult to find. Storm-track reorganization is an alternative and perhaps complementary mechanism to reorganization of thermohaline circulations (Weaver et al. 1991; Kaspi et al. 2004) and sea ice switches (Gildor and Tziperman 2003) for explaining the record of abrupt climate change.

We find that baroclinic adjustment in a wide channel occurs by the formation of multiple narrow jets, each of which while stable supports a substantial fraction of the mean thermal gradient. Moreover, the heat flux across the channel is controlled by these narrow jets.

This work provides a detailed physical theory for the emergence of jet structure and structural transition in baroclinic turbulence. The equilibrium state obtained constitutes a theory for the general circulation of the midlatitude atmosphere.

For reasons of theoretical clarity, we have chosen to concentrate on the case of jets in meridionally homogeneous domains. However, the meridional structure of the earth's subtropical jet is forced and this jet would exist even in the absence of eddies (Held and Hou 1980). Extension of this work to address jet structure and transition when a large-scale meridional structure is imposed will be the subject of future work.

Acknowledgments. This work was supported by NSF ATM-0736022. Petros Ioannou has been partially supported by an ELKE grant by the University of Athens and by the European Social Fund and National Resources–(EPEAEK II)–PYTHAGORAS.

APPENDIX

The Reynolds Matrix

The perturbation equations governing the evolution of the (x, y, z) perturbation velocities (u, v, w) and pressure (p) of the harmonic form

$$(u, v, w, p) = [\hat{u}(t), \hat{v}(t), \hat{w}(t), \hat{p}(t)]e^{i(ly+mz)} \quad \text{(A1)}$$

in an unbounded constant shear flow $\alpha z\,\mathbf{i}$ in a frame rotating in the $-\Omega\,\mathbf{j}$ direction are

$$\frac{d\hat{u}}{dt} = -(\alpha - 2\Omega)\hat{w} - \nu(l^2 + m^2)\hat{u}, \quad \text{(A2a)}$$

$$\frac{d\hat{v}}{dt} = -il\hat{p} - \nu(l^2 + m^2)\hat{v}, \quad \text{and} \quad \text{(A2b)}$$

$$\frac{d\hat{w}}{dt} = -im\hat{p} - 2\Omega\hat{u} - \nu(l^2 + m^2)\hat{w}. \quad \text{(A2c)}$$

These equations describe the evolution of x independent perturbations. These perturbations excite roll circulations in the (y, z) plane associated with zonal (x) streaks (Farrell and Ioannou 1993a).

Using the continuity equation, we obtain

$$\hat{p} = \frac{2im\Omega}{l^2 + m^2}\hat{u}, \quad \text{(A3)}$$

and by eliminating the pressure from the vertical (z) velocity equation, we obtain the dynamical system

$$\frac{d\hat{u}}{dt} = -\nu(l^2 + m^2)\hat{u} - (\alpha - 2\Omega)\hat{w} \quad \text{and} \quad \text{(A4a)}$$

$$\frac{d\hat{w}}{dt} = -\frac{2l^2\Omega}{l^2 + m^2}\hat{u} - \nu(l^2 + m^2)\hat{w}. \quad \text{(A4b)}$$

For constant parameters, the perturbation dynamics are governed by the matrix

$$\mathbf{A} = \begin{bmatrix} -\nu(l^2 + m^2) & -(\alpha - 2\Omega \\ -2\Omega l^2/(l^2 + m^2) & -\nu(l^2 + m^2) \end{bmatrix}. \quad \text{(A5)}$$

The dynamics are stable if the shear of the mean flow is smaller than $\alpha_c = 2\Omega + \nu^2(l^2 + m^2)^3/(2\Omega l^2)$.

When the dynamics are stable, the ensemble mean energy density for unit mass density $\langle E\rangle = \langle \hat{u}^2 + \hat{v}^2 + \hat{w}^2\rangle/4$

maintained under white stochastic excitation with unit covariance is

$$\langle E\rangle = \frac{1}{4}\left(C_{11} + \frac{l^2+m^2}{l^2}C_{22}\right), \tag{A6}$$

where the perturbation covariance matrix $\mathbf{C} = \langle(\hat{u},\hat{w})(\hat{u},\hat{w})^\dagger\rangle$ solves the Lyapunov equation

$$\mathbf{AC} + \mathbf{CA}^\dagger = -\mathbf{I}. \tag{A7}$$

The solution is

$$C_{11} = \frac{2\nu^2(l^2+m^2)^3 - 2fl^2(\alpha-2\Omega) + (\alpha-2\Omega)^2(l^2+m^2)}{8\nu^3(l^2+m^2)^4}E_n, \tag{A8a}$$

$$C_{22} = \frac{\nu^2(l^2+m^2)^4 - \Omega l^2(\alpha-2\Omega)(l^2+m^2) + \Omega^2 l^4}{4\nu^3(l^2+m^2)^5}E_n, \quad \text{and} \tag{A8b}$$

$$C_{12} = C_{21} = -\frac{\alpha(l^2+m^2)+2\Omega l^2}{8\nu^2(l^2+m^2)^3}E_n, \text{ where} \tag{A8c}$$

$$E_n = \frac{\nu(l^2+m^2)^2}{\nu^2(l^2+m^2)^3 - 2\Omega l^2(\alpha-2f)} \tag{A9}$$

is the total variance maintained by the equivalent normal system

$$\mathbf{A}_n = \begin{bmatrix} -\nu\left(l^2+m^2\right) + \sqrt{2\Omega l^2\left(\alpha-2\Omega\right)}\Big/\sqrt{l^2+m^2} & 0 \\ 0 & -\nu\left(l^2+m^2\right) - \sqrt{2\Omega l^2\left(\alpha-2\Omega\right)}\Big/\sqrt{l^2+m^2} \end{bmatrix}, \tag{A10}$$

which has the same eigenvalues as (A5).

As the shear α increases, the equivalent normal total variance E_n increases only in the neighborhood of the critical shear α_c, where the system becomes unstable (see Fig. 9). The nonnormality of the Reynolds matrix is responsible for the power-law behavior of the maintained variance and the flux. Except in the immediate neighborhood of α_c, as α increases, $\langle\hat{u}^2\rangle = C_{11}$ increases proportional to α^2, $\langle\hat{w}^2\rangle = l^2\langle\hat{v}^2\rangle/m^2 = C_{22}$ increases proportional to α, and $\langle\overline{uw}\rangle = C_{12}/2$ increases also proportional to α.

REFERENCES

Alley, R. B., and Coauthors, 1993: Abrupt increase in Greenland snow accumulation at the end of the Younger Dryas event. *Nature,* **362,** 527–529, doi:10.1038/362527a0.

Baldwin, M. P., and Coauthors, 2001: The quasi-biennial oscillation. *Rev. Geophys.,* **39,** 179–229.

Barry, L., G. C. Craig, and J. Thuburn, 2002: Poleward heat transport by the atmospheric heat engine. *Nature,* **415,** 774–777.

Bobba, K. M., B. Bamieh, and J. C. Doyle, 2007: Highly optimized transitions to turbulence. *Proc. 41st Conf. on Decision and Control,*, Las Vegas, NV, IEEE, 4559–4562.

Cehelsky, P., and K. K. Tung, 1991: Nonlinear baroclinic adjustment. *J. Atmos. Sci.,* **48,** 1930–1947.

Chen, G., I. M. Held, and W. A. Robinson, 2007: Sensitivity of the latitude of the surface westerlies to surface friction. *J. Atmos. Sci.,* **64,** 2899–2915.

Cho, J. Y.-K., and L. M. Polvani, 1996: The morphogenesis of bands and zonal winds in the atmospheres on the giant outer planets. *Science,* **273,** 335–337.

Conrath, B. J., P. J. Gierasch, and S. S. Leroy, 1990: Temperature and circulation in the stratosphere of the outer planets. *Icarus,* **83,** 255–281.

DelSole, T., 1996: Can quasigeostrophic turbulence be modeled stochastically? *J. Atmos. Sci.,* **53,** 1617–1633.

——, 1999: Stochastic models of shear-flow turbulence with enstrophy transfer to subgrid scales. *J. Atmos. Sci.,* **56,** 3692–3703.

——, 2004a: The necessity of instantaneous optimals in stationary turbulence. *J. Atmos. Sci.,* **61,** 1086–1091.

——, 2004b: Stochastic models of quasigeostrophic turbulence. *Surv. Geophys.,* **25,** 107–149.

——, 2007: Optimal perturbations in quasigeostrophic turbulence. *J. Atmos. Sci.,* **64,** 1350–1364.

——, and B. F. Farrell, 1995: A stochastically excited linear system as a model for quasigeostrophic turbulence: Analytic results for one- and two-layer fluids. *J. Atmos. Sci.,* **52,** 2531–2547.

——, and ——, 1996: The quasi-linear equilibration of a thermally maintained, stochastically excited jet in a quasigeostrophic model. *J. Atmos. Sci.,* **53,** 1781–1797.

Farrell, B. F., 1982: The initial growth of disturbances in a baroclinic flow. *J. Atmos. Sci.,* **39,** 1663–1686.

——, 1985: Transient growth of damped baroclinic waves. *J. Atmos. Sci.,* **42,** 2718–2727.

——, 1989: Optimal excitation of baroclinic waves. *J. Atmos. Sci.,* **46,** 1193–1206.

——, and P. J. Ioannou, 1993a: Optimal excitation of three-dimensional perturbations in viscous constant shear flow. *Phys. Fluids,* **5,** 1390–1400.

——, and ——, 1993b: Perturbation growth in shear flow exhibits universality. *Phys. Fluids,* **5,** 2298–2300.

——, and ——, 1993c: Stochastic dynamics of baroclinic waves. *J. Atmos. Sci.,* **50,** 4044–4057.

——, and ——, 1993d: Stochastic forcing of the linearized Navier–Stokes equations. *Phys. Fluids,* **5,** 2600–2609.

——, and ——, 1994: A theory for the statistical equilibrium energy spectrum and heat flux produced by transient baroclinic waves. *J. Atmos. Sci.,* **51,** 2685–2698.

——, and ——, 1995: Stochastic dynamics of the midlatitude atmospheric jet. *J. Atmos. Sci.,* **52,** 1642–1656.

——, and ——, 1996: Generalized stability theory. Part I: Autonomous operators. *J. Atmos. Sci.,* **53,** 2025–2040.

——, and ——, 2003: Structural stability of turbulent jets. *J. Atmos. Sci.,* **60,** 2101–2118.

——, and ——, 2007: Structure and spacing of jets in barotropic turbulence. *J. Atmos. Sci.,* **64,** 3652–3665.

Frierson, D. M. W., 2006: Robust increases in midlatitude static stability in simulations of global warming. *Geophys. Res. Lett.,* **33,** L24816, doi:10.1029/2006GL027504.

Fuhrer, K., E. W. Wolff, and S. J. Johnsen, 1999: Timescales for dust variability in the Greenland Ice Core Project (GRIP) ice core in the last 100,000 years. *J. Geophys. Res.,* **104,** 31 043–31 052.

Galperin, B., H. Nakano, H.-P. Huang, and S. Sukoriansky, 2004: The ubiquitous zonal jets in the atmospheres of giant planets and earth's oceans. *Geophys. Res. Lett.,* **31,** L13303, doi:10.1029/2004GL019691.

Gildor, H., and E. Tziperman, 2003: Sea-ice switches and abrupt climate change. *Philos. Trans. Roy. Soc. London,* **361B,** 1935–1944.

Green, J. S. A., 1970: Transfer properties of the large-scale eddies and the general circulation of the atmospheres. *Quart. J. Roy. Meteor. Soc.,* **96,** 157–185.

Gutowski, W. J., Jr., 1985: Baroclinic adjustment and midlatitutde temperature profiles. *J. Atmos. Sci.,* **42,** 1733–1745.

——, L. E. Branscome, and D. A. Stewart, 1989: Mean flow adjustment during life cycles of baroclinic waves. *J. Atmos. Sci.,* **46,** 1724–1737.

Haidvogel, D. B., and I. Held, 1980: Homogeneous quasigeostrophic turbulence driven by a uniform temperature gradient. *J. Atmos. Sci.,* **37,** 2644–2660.

Hall, N. M. J., and P. D. Sardeshmukh, 1998: Is the time-mean Northern Hemisphere flow baroclinically unstable? *J. Atmos. Sci.,* **55,** 41–56.

Held, I. M., 1978: The vertical scale of an unstable baroclinic wave and its importance for eddy heat flux parameterizations. *J. Atmos. Sci.,* **35,** 572–576.

——, 1982: On the height of the tropopause and the static stability of the troposphere. *J. Atmos. Sci.,* **39,** 412–417.

——, 1999: The macroturbulence of the troposphere. *Tellus,* **51,** 59–70.

——, and A. Y. Hou, 1980: Nonlinear axially symmetric circulations in a nearly inviscid atmosphere. *J. Atmos. Sci.,* **37,** 515–533.

——, and V. D. Larichev, 1996: A scaling theory for horizontally homogeneous, baroclinically unstable flow on a beta plane. *J. Atmos. Sci.,* **53,** 946–952.

Huang, H.-P., and W. A. Robinson, 1998: Two-dimensional turbulence and persistent zonal jets in a global barotropic model. *J. Atmos. Sci.,* **55,** 611–632.

Ingersoll, A. P., 1990: Atmospheric dynamics of the outer planets. *Science,* **248,** 308–315.

Ioannou, P. J., 1995: Nonnormality increases variance. *J. Atmos. Sci.,* **52,** 1155–1158.

——, and R. S. Lindzen, 1986: Baroclinic instability in the presence of barotropic jets. *J. Atmos. Sci.,* **43,** 2999–3014.

James, I. N., 1987: Suppression of baroclinic instability in horizontally sheared flows. *J. Atmos. Sci.,* **44,** 3710–3720.

Jeffreys, H., 1933: The function of cyclones in the general circulation. *Proc. Verbaux de l'Association de Meteorologie, Part II,* Lisbon, Portugal, UGGI, 219–230.

Juckes, M. N., 2000: The static stability of the midlatitude troposphere: The relevance of moisture. *J. Atmos. Sci.,* **57,** 3050–3057.

Kaspi, Y. H., and G. R. Flierl, 2007: Formation of jets by baroclinic instability on gas planet atmospheres. *J. Atmos. Sci.,* **64,** 3177–3194.

——, R. Sayag, and E. Tziperman, 2004: A "triple sea-ice state" mechanism for the abrupt warming and synchronous ice sheet collapses during Heinrich events. *Paleoceanography,* **19,** PA3004, doi:10.1029/2004PA001009.

Krishnamurti, R., and L. N. Howard, 1981: Large-scale flow generation in turbulent convection. *Proc. Natl. Acad. Sci. USA,* **78,** 1981–1985.

Lapeyre, G., and I. M. Held, 2003: Diffusivity, kinetic energy dissipation, and closure theories for the poleward eddy heat flux. *J. Atmos. Sci.,* **60,** 2907–2916.

Lee, S., 1997: Maintenance of multiple jets in a baroclinic flow. *J. Atmos. Sci.,* **54,** 1726–1738.

——, 2005: Baroclinic multiple jets on the sphere. *J. Atmos. Sci.,* **62,** 2484–2498.

——, and H. Kim, 2003: The dynamical relationship between subtropical and eddy-driven jets. *J. Atmos. Sci.,* **60,** 1490–1503.

Li, C., and D. S. Battisti, 2008: Reduced Atlantic stormines during the last glacial maximum: Evidence from a coupled climate model. *J. Climate,* **21,** 3561–3579.

——, ——, D. P. Schrag, and E. Tziperman, 2005: Abrupt climate shifts in Greenland due to displacements of the sea ice edge. *Geophys. Res. Lett.,* **32,** L19702, doi:10.1029/2005GL023492.

Lindzen, R. S., 1993: Baroclinic neutrality and the tropopause. *J. Atmos. Sci.,* **50,** 1148–1151.

——, and B. F. Farrell, 1980: The role of polar regions in global climate, and a new parameterization of global heat transport. *Mon. Wea. Rev.,* **108,** 2064–2079.

MacAyeal, D. R., 1993: Binge/purge oscillations of the Laurentide ice sheet as a cause of the North Atlantic's Heinrich events. *Paleoceanography,* **8,** 775–784.

Manfroi, A. J., and W. R. Young, 1999: Slow evolution of zonal jets on the beta plane. *J. Atmos. Sci.,* **56,** 784–800.

Maximenko, N. A., B. Bang, and H. Sasaki, 2005: Observational evidence of alternating zonal jets in the World Ocean. *Geophys. Res. Lett.,* **32,** L12607, doi:10.1029/2005GL022728.

Muench, J., and E. Kunze, 1994: The potential vorticity structure of equatorial deep jets. *J. Phys. Oceanogr.,* **24,** 418–428.

Nakamura, H., 1992: Midwinter suppression of baroclinic wave activity in the Pacific. *J. Atmos. Sci.,* **49,** 1629–1642.

Nakano, H., and H. Hasumi, 2005: A series of zonal jets embedded in the broad zonal flows in the Pacific obtained in eddy-permitting Ocean General Circulation Models. *J. Phys. Oceanogr.,* **35,** 474–488.

Newman, M., P. D. Sardeshmukh, and C. Penland, 1997: Stochastic forcing of the wintertime extratropical flow. *J. Atmos. Sci.,* **54,** 435–455.

Nozawa, T., and S. Yoden, 1997: Formation of zonal band struc-

ture in forced two-dimensional turbulence on a rotating sphere. *Phys. Fluids,* **9,** 2081–2093.

Panetta, R. L., 1993: Zonal jets in wide baroclinically unstable regions: Persistence and scale selection. *J. Atmos. Sci.,* **50,** 2073–2106.

——, and I. M. Held, 1988: Baroclinic eddy fluxes in a one-dimensional model of quasigeostrophic turbulence. *J. Atmos. Sci.,* **45,** 3354–3365.

Pavan, P., and I. M. Held, 1996: The diffusive approximation for eddy fluxes in baroclinically unstable jets. *J. Atmos. Sci.,* **53,** 1262–1272.

Phillips, N. A., 1954: Energy transformations and meridional circulations associated with simple baroclinic waves in a two-level, quasigeostrophic model. *Tellus,* **6,** 273–286.

Read, P. L., Y. H. Yamazaki, S. R. Lewis, P. D. Williams, K. Miki-Yamazaki, J. Sommeria, H. Didelle, and A. Fincham, 2004: Jupiter's and Saturn's convectively driven banded jets in the laboratory. *Geophys. Res. Lett.,* **31,** L22701, doi:10.1029/2004GL020106.

——, ——, ——, ——, R. Wordsworth, K. Miki-Yamazaki, J. Sommeria, and H. Didelle, 2007: Dynamics of convectively driven banded jets in the laboratory. *J. Atmos. Sci.,* **64,** 4031–4052.

Rhines, P. B., 1975: Waves and turbulence on a beta plane. *J. Fluid Mech.,* **69,** 417–433.

Richards, K. J., N. A. Maximenko, F. O. Bryan, and H. Sasaki, 2006: Zonal jets in the Pacific Ocean. *Geophys. Res. Lett.,* **33,** L03605, doi:10.1029/2005GL024645.

Robinson, W. A., 2006: On the self-maintenance of midlatitude jets. *J. Atmos. Sci.,* **63,** 2109–2122.

Roe, G. H., and R. S. Lindzen, 1996: Baroclinic adjustment in a two-level model with barotropic shear. *J. Atmos. Sci.,* **53,** 2749–2754.

Sánchez-Lavega, A., and Coauthors, 2008: Depth of a strong Jovian jet from a planetary-scale disturbance driven by storms. *Nature,* **451,** 437–440.

Sarachik, E. S., 1985: A simple theory for the vertical structure of the tropical atmosphere. *Pure Appl. Geophys.,* **123,** 261–271.

Sardeshmukh, P. D., and P. Sura, 2007: Multiscale impacts of variable heating in climate. *J. Climate,* **20,** 5677–5695.

Schneider, T., and C. C. Walker, 2006: Self-organization of atmospheric macroturbulence into critical states of weak nonlinear eddy–eddy interactions. *J. Atmos. Sci.,* **63,** 1569–1586.

Stone, P. H., 1972: A simplified radiative–dynamical model for the static stability of rotating atmospheres. *J. Atmos. Sci.,* **29,** 405–418.

——, 1974: The meridional variation of the eddy heat fluxes by baroclinic waves and their parameterization. *J. Atmos. Sci.,* **31,** 444–456.

——, 1978: Baroclinic adjustment. *J. Atmos. Sci.,* **35,** 561–571.

——, and D. A. Miller, 1980: Empirical relations between seasonal changes in meridional temperature gradients and meridional fluxes of heat. *J. Atmos. Sci.,* **37,** 1708–1721.

——, and L. Branscome, 1992: Diabatically forced, nearly inviscid eddy regimes. *J. Atmos. Sci.,* **49,** 355–367.

Toggweiler, J. R., J. L. Russell, and S. R. Carson, 2006: Midlatitude westerlies, atmospheric CO_2, and climate change during the ice ages. *Paleoceanography,* **21,** PA2005, doi:10.1029/2005PA001154.

Vallis, G. K., 2006: *Atmospheric and Oceanic Fluid Dynamics: Fundamentals and Large-Scale Circulation.* Cambridge University Press, 745 pp.

——, and M. E. Maltrud, 1993: Generation of mean flows and jets on a beta plane and over topography. *J. Phys. Oceanogr.,* **23,** 1346–1362.

Vasavada, A. R., and A. P. Showman, 2005: Jovian atmospheric dynamics: An update after *Galileo* and *Cassini*. *Rep. Prog. Phys.,* **68,** 1935–1996.

Weaver, A. J., E. S. Sarachik, and J. Marotze, 1991: Freshwater flux forcing of decadal and interdecadal oceanic variability. *Nature,* **353,** 836–838.

Welch, W. T., and K.-K. Tung, 1998: Nonlinear baroclinic adjustment and wavenumber selection in a simple case. *J. Atmos. Sci.,* **55,** 1285–1302.

Whitaker, J. S., and P. D. Sardeshmukh, 1998: A linear theory of extratropical synoptic eddy statistics. *J. Atmos. Sci.,* **55,** 237–258.

Williams, G. P., 1979: Planetary circulations: 2. The Jovian quasi-geostrophic regime. *J. Atmos. Sci.,* **36,** 932–968.

——, 2003: Jet sets. *J. Meteor. Soc. Japan,* **81,** 439–476.

Wunsch, C., 2003: Greenland–Antarctic phase relations and millennial time-scale climate fluctuations in the Greenland ice-cores. *Quat. Sci. Rev.,* **22,** 1631–1646.

Xu, K.-M., and K. A. Emanuel, 1989: Is the tropical atmosphere conditionally unstable? *Mon. Wea. Rev.,* **117,** 1471–1479.

Yamazaki, Y. H., D. R. Skeet, and P. L. Read, 2004: A new general circulation model of Jupiter's atmosphere based on the UKMO Unifed Model: Three-dimensional evolution of isolated vortices and zonal jets in mid-latitudes. *Planet. Space Sci.,* **52,** 423–445.

Zhang, Y., and I. M. Held, 1999: A linear stochastic model of a GCM's midlatitude storm tracks. *J. Atmos. Sci.,* **56,** 3416–3435.

Zhou, K., and J. C. Doyle, 1998: *Essentials of Robust Control.* Prentice Hall, 411 pp.

Zhou, S., and P. H. Stone, 1993: The role of large-scale eddies in the climate equilibrium. Part I: Fixed static stability. *J. Climate,* **6,** 985–1001.

Zurita-Gotor, P., 2007: The relation between baroclinic adjustment and turbulent diffusion in the two-layer model. *J. Atmos. Sci.,* **64,** 1284–1300.

——, and R. S. Lindzen, 2004a: Baroclinic equilibration and the maintenance of the momentum balance. Part I: A barotropic analog. *J. Atmos. Sci.,* **61,** 1469–1482.

——, and R. S. Lindzen, 2004b: Baroclinic equilibration and the maintenance of the momentum balance. Part II: 3D results. *J. Atmos. Sci.,* **61,** 1483–1499.